AD-F300213

AD A126103

AD

CONTRACT REPORT ARBRL-CR-00506

MUZZLE FLASH ONSET: AN ALGEBRAIC CRITERION AND FURTHER VALIDATION OF THE MUZZLE EXHAUST FLOW FIELD MODEL

Prepared by

Aerodyne Research, Inc.
The Research Center at Manning Park
45 Manning Road
Billerica, MA 01821

DTIC
MAR 15

March 1983

US ARMY ARMAMENT RESEARCH AND DEVELOPMENT COMMAND
BALLISTIC RESEARCH LABORATORY
ABERDEEN PROVING GROUND, MARYLAND

Approved for public release; distribution unlimited.

DTIC FILE COPY

83 03 14 109

Destroy this report when it is no longer needed.
Do not return it to the originator.

Additional copies of this report may be obtained from the National Technical Information Service, U. S. Department of Commerce, Springfield, Virginia 22161.

The findings in this report are not to be construed as an official Department of the Army position, unless so designated by other authorized documents.

The use of trade names or manufacturers' names in this report does not constitute indorsement of any commercial product.

UNCLASSIFIED

SECURITY CLASSIFICATION OF THIS PAGE *(When Data Entered)*

REPORT DOCUMENTATION PAGE		READ INSTRUCTIONS BEFORE COMPLETING FORM
1. REPORT NUMBER CONTRACT REPORT ARBRL-CR-00506	2. GOVT ACCESSION NO. AD-A126 103	3. RECIPIENT'S CATALOG NUMBER
4. TITLE *(and Subtitle)* MUZZLE FLASH ONSET: AN ALGEBRAIC CRITERION AND FURTHER VALIDATION OF THE MUZZLE EXHAUST FLOW FIELD MODEL		5. TYPE OF REPORT & PERIOD COVERED Final Report May 1981 - January 1982
		6. PERFORMING ORG. REPORT NUMBER ARI-RR-296
7. AUTHOR*(s)* V. Yousefian		8. CONTRACT OR GRANT NUMBER*(s)* DAAK11-78-C-0107
9. PERFORMING ORGANIZATION NAME AND ADDRESS Aerodyne Research, Inc. The Research Center at Manning Park 45 Manning Road, Billerica, MA 01821		10. PROGRAM ELEMENT, PROJECT, TASK AREA & WORK UNIT NUMBERS 1L161102AH43
11. CONTROLLING OFFICE NAME AND ADDRESS US Army Armament Research & Development Command US Army Ballistic Research Laboratory (DRDAR-BL) Aberdeen Proving Ground, MD 21005		12. REPORT DATE March 1983 13. NUMBER OF PAGES 63
14. MONITORING AGENCY NAME & ADDRESS*(if different from Controlling Office)*		15. SECURITY CLASS. *(of this report)* UNCLASSIFIED 15a. DECLASSIFICATION/DOWNGRADING SCHEDULE

16. DISTRIBUTION STATEMENT *(of this Report)*

Approved for public release; distribution unlimited.

17. DISTRIBUTION STATEMENT *(of the abstract entered in Block 20, if different from Report)*

18. SUPPLEMENTARY NOTES

19. KEY WORDS *(Continue on reverse side if necessary and identify by block number)*

Muzzle flash
Suppression chemistry

20. ABSTRACT *(Continue on reverse side if necessary and identify by block number)*

In this report an algebraic criterion to predict the onset of muzzle flash is formulated. The criterion is derived from the detailed analysis of a complex Muzzle Exhaust Flow Field (MEFF) model which includes turbulence and detailed chemical kinetics. The algebraic criterion, therefore, contains the essential features of the complex MEFF model. Additional efforts required for the improvement of the criterion are discussed.

DD FORM 1 JAN 73 1473 EDITION OF 1 NOV 65 IS OBSOLETE

UNCLASSIFIED

SECURITY CLASSIFICATION OF THIS PAGE *(When Data Entered)*

The validity of the MEFF model is further demonstrated by comparing its flash onset predictions with those of observations for several gun systems. A sensitivity analysis is performed to determine the dependence of the prediction on variations in certain key parameters (e.g., chemical rate constant).

TABLE OF CONTENTS

1. INTRODUCTION

Muzzle flash is an undesirable, but often inevitable, by-product of the use of firearms. The occurrence of extensive muzzle flash results in easy detection, causes loss of night vision in the gun crew, and can substantially increase blast overpressures. Muzzle flash can in general be eliminated by the use of chemical suppressants. The effective use of such chemicals, however, requires a thorough understanding of the many phenomena that are responsible for the onset of muzzle flash. In the present context, muzzle flash refers to the secondary combustion of the fuel-rich gun exhaust gases after mixing with air.

The first systematic approach towards the development of a muzzle flash methodology was described by Carfagno.[1] In this approach the muzzle flash flow field was reduced to a simple one-dimensional instantaneous mixing analysis. The results of complex chemical reactions were reduced to experimentally determined ignition temperatures. Mixing with ambient air was treated in an ad hoc fashion. Flash could be expected if the shock-heated muzzle gas-air mixture temperature exceeded the experimental ignition limits. After clearing up some minor details and inconsistencies in Carfagno's approach, May and Einstein[2] improved this methodology by using a more realistic interior ballistic model. When applied to a large caliber gun, this approach resulted in a satisfactory a priori prediction of the muzzle flash onset. The applicability of this model, however, is somewhat limited since it requires the experimentally determined ignition temperature for each new propellant. We need a model, therefore, which incorporates the basic flow and chemical phenomena which lead to muzzle flash.

DTIC COPY INSPECTED 2

Accession For
NTIS GRA&I
DTIC TAB
Unannounced
Justification
By
Distribution/
Availability Codes
Dist | Avail and/or Special
A

We have considered a muzzle flash model that integrates an interior ballistic model and an axisymmetric, turbulent, quasi-steady exhaust flow field model and couples detailed, complex chemical reaction kinetics. We have previously reported[3,4] a muzzle exhaust flow field model that incorporates a chemical reaction scheme suggested by Jensen and Jones[5] and a turbulent mixing model described by Mikatarian et al.[6] When applied to the same large caliber gun flash problem described by May and Einstein[2] good agreement with experimental results were achieved.

The complexity of the muzzle exhaust flow model described in Reference 3 is considerable. This is mainly due to the turbulent and reacting nature of the flow field where secondary combustion occurs. By the careful examination of several computed results, it became apparent that the ignition process, and hence the onset of muzzle flash, may be represented by a significantly simpler model without losing the phenomenology associated with turbulent mixing and chemical kinetics. One objective of this report is the description of this simpler model. In Section 2, the basic elements of the muzzle exhaust flow field and chemical kinetics models are reviewed. The model predictions are discussed in Section 3 where the feasibilty of developing a simpler model is also deduced. Section 4 contains the formulation of the simple model and its potential for predicting the muzzle flash onset.

The predictions of the analytical model are at best as accurate as those of the more complex Muzzle Exhaust Flow Field (MEFF) model. The validity of the MEFF model has been tested for a single gun system using three different propellant compositions. For all three cases the predicted results agreed with those of observation. To further validate the predictive capability of the MEFF model, in Section 5 we have compared the flash/no-flash predictions of the MEFF model with those of observation for five additional gun propellant systems. Within the sensitivity limits of the model, the predicted and observed flash data agree.

To a large extent, the flash/no-flash predictions of the MEFF model depend on a variety of input variables (e.g., reaction rate constants, species thermodynamic data, muzzle properties, etc.). The values of these variables, however, are not known accurately. To determine the dependence of the predicted results on variations in the nominal value of some important input variables, a sensitivity analysis is performed in Section 6. The conclusions and recommendations are considered in Section 7.

2. MUZZLE EXHAUST FLOW AND CHEMISTRY MODEL

A full description of muzzle exhaust fluid dynamic and chemical kinetics models are given in References 3 and 4. These reports also contain the references which are used to develop the muzzle exhaust flow field model. In this section the basic elements of the model are described.

MUZZLE EXHAUST FLOW MODEL

The muzzle exhaust flow field after the ejection of the projectile is shown schematically in Figure 1. It is comprised of a blast wave, downstream of which ambient conditions exist, and three distinct flow regions. These are the flow in the gun barrel (i.e., the interior ballistics), the expansion region, typical of highly underexpanded jets, and the turbulent mixing region where afterburning occurs as a result of propellant/air mixing. The muzzle conditions are required to determine a unique solution for the expansion region. Then, the conditions along the boundary of the expansion and mixing regions are required to get a unique solution for the afterburning region. For muzzle flash onset predictions, the blast wave is neglected here. The methodology used to evaluate the required boundary conditions is described elsewhere.[3,4]

One of the parameters required to determine the afterburning region boundary conditions is the normal shock radius shown in Figure 1. In our previous attempt, semi-empirical results were used to estimate the size of the normal shock. The semi-empirical results, however, were based on underexpanded jets with pressure ratios considerably less than those of muzzle exhaust flows. In a recent paper Schmidt[7] has reported that the observed normal shock radius of muzzle exhausts is greater than our previous estimate. To be consistent with observation, in this paper the larger radius, estimated by Schmidt,[7] will be used. The result yields a mixing region boundary

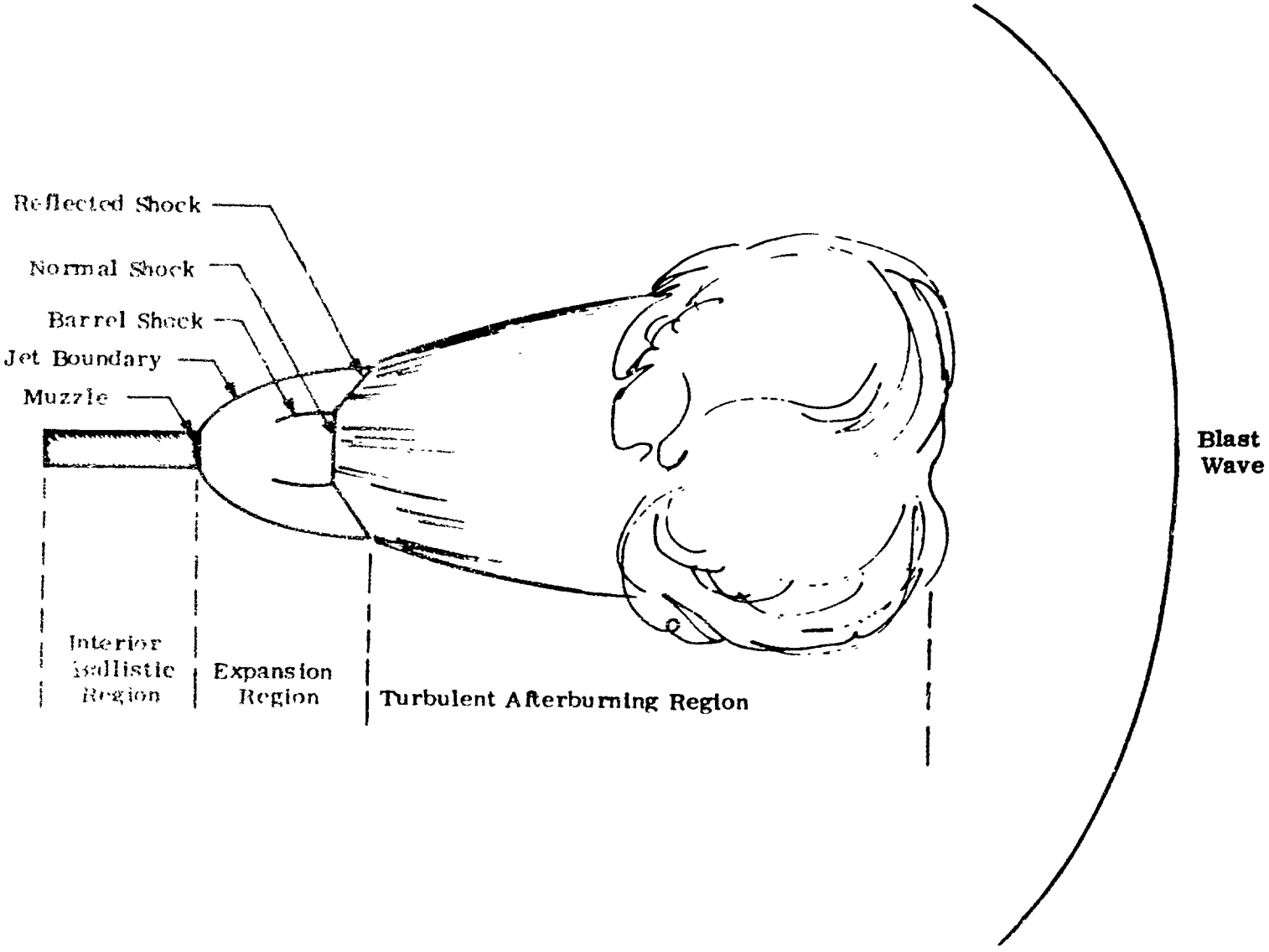

Figure 1. Schematic Diagram of Muzzle Flash Flow Regions

temperature (velocity) which is larger (smaller) than the one derived in Ref. 3.

Using the larger normal shock radius and the flow field model described above and elsewhere,[3,4] the mixing region boundary conditions were calculated for a basic propellant designated M30Al and containing 2.5, 5 and 6 percent K_2SO_4 as chemical suppressant. The result is shown in Table 1. The flow field generated by these propellants is analyzed in the next section to determine if simpler models can be developed for predicting muzzle flash onset.

AFTERBURNING CHEMISTRY

Elementary chemical reactions have been explicitly incorporated in this modeling effort. The reactions and their rate constants are listed in Table 2. Reverse rate constants are automatically generated by the computational procedure used in this study. The references for the rate constants of Table 2 are given in Reference 4. In a recent paper, Jensen and Jones[8] have used the same set of reactions to investigate the effects of chemical suppressants on rocket exhaust flow fields.

The thermodynamic data of the species comprising the mixture are required to determine both the thermodynamic properties of the gas and the reverse rate constants of the reactions used. Except for KO_2 and HO_2 the JANAF[9] thermodynamic tables are used to specify the data for the species appearing in Table 1. The HO_2 heat of formation adopted is that indicated by the recent work of Howard.[10]

The KO_2 heat of formation used by Jensen and Jones[8] is based on the dissociation energy of NaO_2. From the information given in their paper, a dissociation energy of about 55 kcal/mole can be deduced for KO_2. This is close to the value of NaO_2 dissociation energy reported by Dougherty et al.[11] In a recent paper Alexander[12] has shown that the NaO_2 dissociation energy is

Table 1. Calculated Mixing Region Boundary Conditions (M30Al Propellant With K_2SO_4 Suppressant)

Percent Suppressant		2.5	5	6
Mixing Region Boundary T(K)		1018	1018	1018
Mixing Region Boundary P(Atm)		1	1	1
Mixing Region Boundary U(m/sec)		1888	1888	1888
Mixing Region Boundary Mole Fraction				
1.	H	6.887(-5)	6.695(-5)	4.831(-5)
2.	O	1.434(-8)	1.546(-8)	6.964(-9)
3.	OH	8.893(-6)	9.310(-6)	6.165(-6)
4.	HO_2	<1.000(-12)	<1.000(-12)	<1.000(-12)
5.	KO_2	<1.000(-12)	<1.000(-12)	<1.000(-12)
6.	H_2	1.473(-1)	1.340(-1)	1.321(-1)
7.	O_2	1.000(-9)	1.162(-8)	5.267(-9)
8.	N_2	2.756(-1)	2.745(-1)	2.827(-1)
9.	KOH	5.937(-3)	1.219(-2)	1.427(-2)
10.	CO	2.492(-1)	2.438(-1)	2.388(-1)
11.	CO_2	9.579(-2)	9.979(-2)	1.037(-1)
12.	H_2O	2.253(-1)	2.280(-1)	2.264(-1)
13.	K	8.758(-4)	1.744(-3)	1.900(-3)

Table 2. Elementary Reactions

	Reaction	Forward Rate Constant*	Uncertainty Factor
1.	$CO + O + M = CO_2 + M$	$0.70(-32)\ \exp(-4369/RT)$	30
2.	$CO + O_2 = CO_2 + O$	$0.42(-11)\ \exp(-47664/RT)$	3
3.	$CO + OH = CO_2 + H$	$0.28(-16)\ T^{1.3}\ \exp(660/RT)$	3
4.	$O + O + M = O_2 + M$	$0.30(-33)\ \exp(1792/RT)$	10
5.	$OH + H_2 = H_2O + H$	$0.19(-14)\ T^{1.3}\ \exp(-3626/RT)$	2
6.	$H + O_2 = OH + O$	$0.24(-9)\ \exp(-16393/RT)$	1.5
7.	$O + H_2 = OH + H$	$0.30(-13)\ T\ \exp(-8902/RT)$	1.5
8.	$OH + OH = H_2O + O$	$0.10(-10)\ \exp(-1093/RT)$	3
9.	$H + H + M = H_2 + M$	$0.30(-29)\ T^{-1}$	30
10.	$H + OH + M = H_2O + M$	$0.10(-24)\ T^{-2}$	10
11.	$H + O_2 + M = HO_2 + M$	$0.15(-31)\ \exp(994/RT)$	3
12.	$H + HO_2 = OH + OH$	$0.17(-9)\ \exp(-994/RT)$	4
13.	$CO + HO_2 = CO_2 + OH$	$0.25(-9)\ \exp(-23645/RT)$	3
14.	$H + HO_2 = H_2 + O_2$	$0.42(-10)\ \exp(-695/RT)$	3
15.	$H + HO_2 = H_2O + O$	$0.85(-11)\ \exp(-994/RT)$	5
16.	$OH + HO_2 = H_2O + O_2$	$0.30(-10)$	3
17.	$O + HO_2 = OH + O_2$	$0.35(-10)$	3
18.	$H + KOH = H_2O + K$	$0.18(-10)\ \exp(-1987/RT)$	3
19.	$K + OH + M = KOH + M$	$0.15(-26)\ T^{-1}$	2.5
20.	$O + H + M = OH + M$	$0.10(-28)\ T^{-1}$	30
21.	$KO_2 + OH = KOH + O_2$	$0.20(-10)$	30
22.	$K + O_2 + M = KO_2 + M$	$0.30(-29)\ T^{-1}$	10
23.	$HO_2 + H_2 = H_2O + OH$	$0.10(-11)\ \exp(-18678/RT)$	10
24.	$K + HO_2 = KO_2 + H$	$0.10(-10)\ \exp(-13000/RT)$	30
25.	$KO_2 + H_2 = KOH + OH$	$0.30(-11)\ \exp(-19870/RT)$	100

*Units of cm-particle-s, read 2.4 (-10) as 2.4×10^{-10}

R=1.987 (cal $mole^{-1}$-K^{-1})

about 36 kcal/mole. Based on the assumption that KO_2 has the same dissociation energy, we were able to estimate a thermodynamic data for KO_2.

Changes in the dissociation energy of KO_2 will significantly affect both the estimated rate constants and the calculated equilibrium constants of reactions containing KO_2. Inspection of KO_2 chemical reactions listed in Table 2 showed that the estimated activation energy of about 2 kcal/mole, used by Jensen and Jones,[8] for reaction 24 is too small to be consistent with the new KO_2 data. The activation energy for a simple endoergic reaction must be at least equal to the difference between the energy of the products and reactants. Using the new KO_2 data, this difference for reaction 24 is about 13 kcal/mole. This is the value listed in Table 2. Utilization of the rate constants listed in Table 2 and the computational model presented in References 3 and 4 does result in muzzle flash/no-flash predictions for several propellants which are consistent with available observations.

3. ANALYSIS OF THE PREDICTED RESULTS

In this section the predicted muzzle exhaust flow field is analyzed for the three-propellant formulation listed in Table 1 to determine if simpler models capable of predicting the muzzle flash onset can be developed.

The numerical procedure used here yields the radial and axial distribution of mixture temperature and species concentration in the afterburning region. Muzzle flash is predicted when there is a sudden jump in the calculated flow temperature. Ignition (i.e., muzzle flash) is initiated at a point where the gas temperature exceeds the propellant-air mixture ignition temperature. Depending on the plume initial conditions (e.g., Mach number, temperature, suppressant amount), the ignition point is somewhere within one initial boundary radius from the plume center line. For example, for the M30A1 propellant with 1% suppressant, the predicted ignition is off the center line in the propellant-air interface. When the amount of suppressant is increased to 2.5% percent, however, ignition is predicted along the center line.

For the cases considered in this section, the predicted temperature jump first occurs along the center line. Figure 2 shows the center line variation of the predicted temperatures generated by the propellants given in Table 1. The abrupt change in the temperature profiles of the propellants with 2.5 and 5 percent suppressants indicate the onset of muzzle flash. The smooth temperature rise and decay for the propellant with 6 percent suppressant shows that flash is suppressed for this case.

An important feature of Figure 2 is the nearly overlapping of the three temperature profiles prior to ignition. This is an indication that prior to ignition, chemistry may not have a significant effect on the bulk properties of the mixture (e.g., the concentration of the major species). The validity of this assertion can be deduced from Figures 3, 4, and 5. These figures show

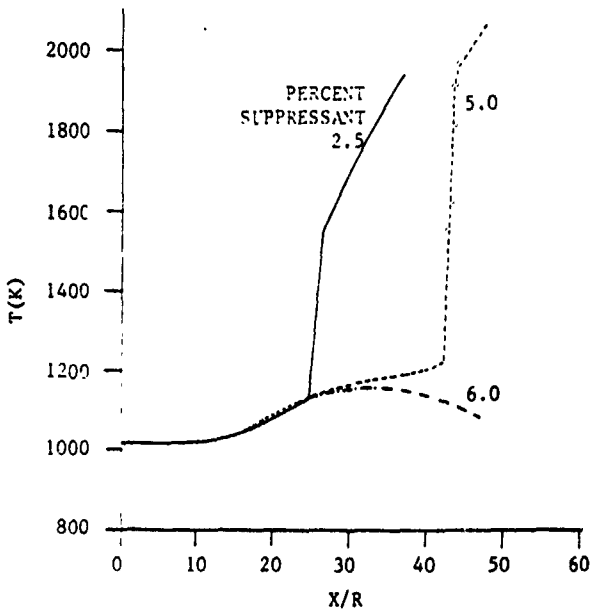

Figure 2. Centerline Temperature vs. Axial Distance and Percent Suppressant.
(R = Initial Boundary Radius)

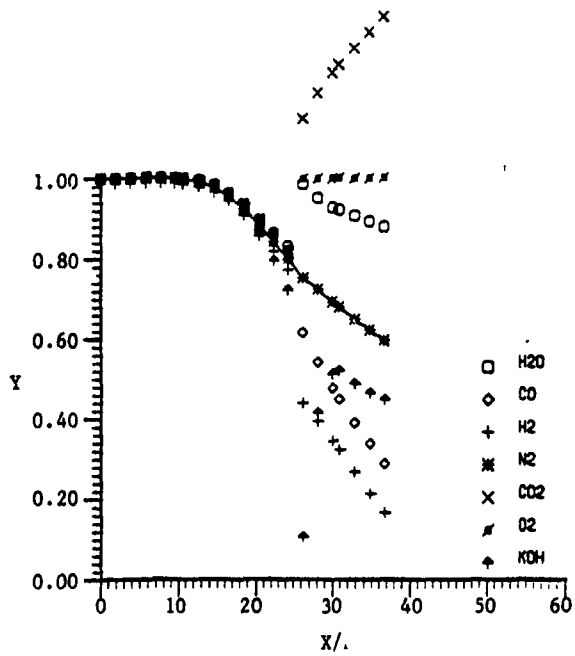

Figure 3. Major Species Normalized Centerline Concentration vs. Axial Distance, 2.5% Suppressant.
(R = Initial Boundary Radius)

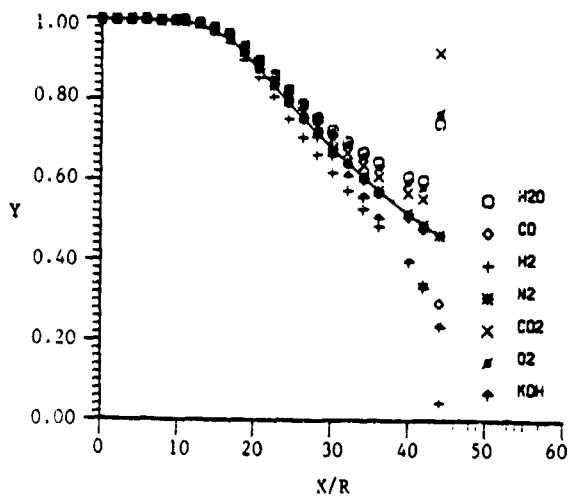

Figure 4. Major Species Normalized Centerline Concentration vs. Axial Distance, 5.0% Suppressant.
(R = Initial Boundary Radius)

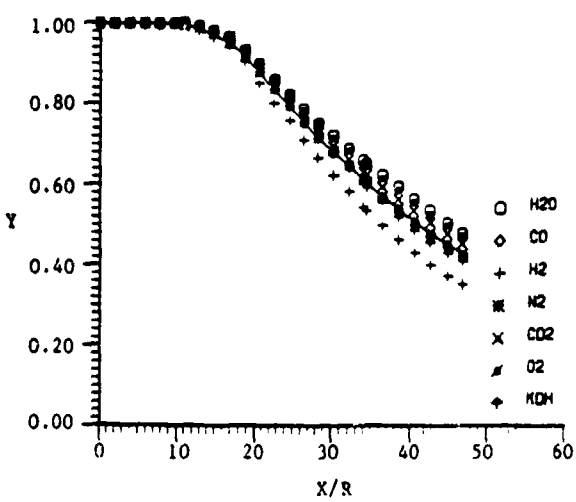

Figure 5. Major Species Normalized Centerline Concentration vs. Axial Distance, 6.0% Suppressant.
(R = Initial Boundary Radius)

the axial profiles of Y_i, the normalized concentration of the i-th major species, for the three cases considered. Here Y_i is defined as:

$$Y_i = \frac{N_i - N_{\infty i}}{N_{oi} - N_{\infty i}} \tag{1}$$

where N_i is the number moles of i-th species per unit mass. Subscripts (o) and (∞) refer to the concentration at the initial boundary and background, respectively. The major species, which comprise over 99 percent of the mixture, are defined to be H_2O, CO, H_2, CO_2, O_2 and KOH.

Inspection of Figures 3 to 5 shows that similar to the temperature variation, the preignition profiles of any Y_i are practically the same for the three propellants considered. In addition, within about 10 percent all the Y_i for a given propellant are the same and equal to that of the chemically inert species N_2. Therefore, turbulent mixing, which is similar for all the species, must govern the predicted preignition variation of each major species concentration.

Therefore, it is concluded that prior to ignition chemistry must only affect the evolution of the minor species which are H, OH, O, K, KO_2, and HO_2. This implies that only an analysis of minor species behavior will indicate the conditions under which muzzle flash can occur.

Figures 6, 7, and 8 show the axial variations of the minor species calculated mole fraction for the cases considered here. The profile of KOH is included for comparison. Reference to Figures 6-8 shows that two distinct flow regions can be defined. In region 1, which extends from $x \approx 0$ to $x \approx 15$, K is converted into KO_2, mainly through reaction 22. In this region the qualitative behavior of the species concentration is common to both suppressed and unsuppressed cases. This indicates that conditions which

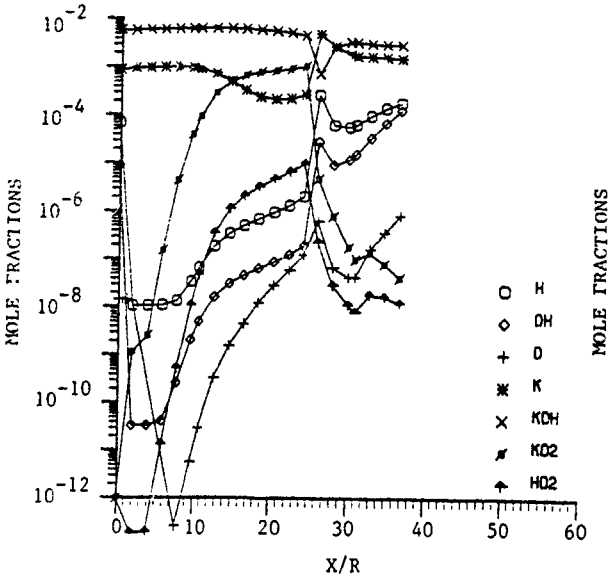

Figure 6. Minor Species Centerline Mole Fractions vs. Axial Distance, 2.5% Suppressant. (R = Initial Boundary Radius)

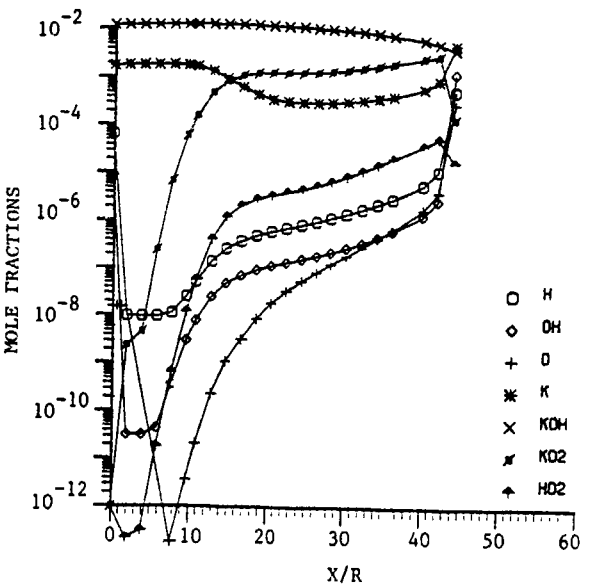

Figure 7. Minor Species Centerline Mole Fractions vs. Axial Distance, 5.0% Suppressant. (R = Initial Boundary Radius)

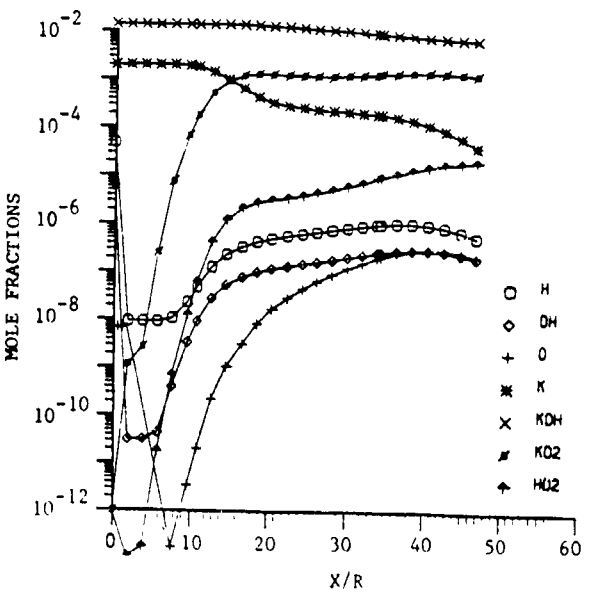

Figure 8. Minor Species Centerline Mole Fractions vs. Axial Distance, 6.0% Suppressant. (R = Initial Boundary Radius)

determine whether flashing will occur are governed by the chemistry taking place in region 2, which extends downstream of x ≃ 15.

To determine the conditions leading to the onset of muzzle flash, we first consider an order of magnitude analysis which shows that in region 2 the variations of the minor species concentration, except KO_2, are mainly controlled by chemistry with turbulent mixing having an insignificant effect. For species such as oxygen atoms, this can be readily deduced from Figures 6-8, which show that the rate of change of oxygen atoms is considerably greater than that of KOH which is controlled by mixing.

The following analysis is valid when the propellant contains suppressant so that regions 1 and 2 can be defined. The analysis considered here must be repeated to determine ignition criterion when the propellant does not contain any suppressant. For suppressant-free cool-burning propellant, flash may be inhibited because of reaction (11) which can be a sink for H radicals.

ORDER OF MAGNITUDE ANALYSIS

The rate of change of species concentration, N_i, is given by its conservation equation which can be written in the following form

$$\frac{1}{N_i}\frac{dN_i}{dt} = \frac{1}{\tau_t} + \frac{1}{\tau_{ic}} \tag{2}$$

where τ_t, the characteristic turbulent mixing time, is the same for all species while τ_{ic}, the characteristic reaction time, depends on the chemical kinetics and can be different for different species. When $\tau_t \ll \tau_{ic}$ turbulence is the dominant phenomenon for change and when $\tau_t \gg \tau_{ic}$ chemistry is.

The turbulent diffusion time constant, τ_t, is of the order of u/x, where u is the center line velocity at the axial station x. For the flow field

considered here, $\tau_t > 10^{-3}$ sec in region 2. The chemical time constant, τ_{ic}, equals to $(N_i/\dot{N}_{ic})$ where $\dot{N}_{ic}$, defined as the net chemical production rate of i-th species, is in general the algebraic sum of terms which are proportional to the product $N_k N_j$. Here, N_k and N_j refer to species appearing in a particular reaction. For the chemical kinetics considered here, detailed analysis has shown that in preignition regions the chemical rates which make a significant contribution to any of the $\dot{N}_{ic}$ are such that at least one of the terms appearing in the $N_k N_j$ product belongs to a minor species. Therefore, for the major species τ_{ic} is inversely proportional to the concentration of one or more minor species. Since prior to ignition the concentration of the minor species is very small, then, unless the reaction rate constants are very large, we expect τ_{ic} to be much greater than τ_t, making turbulence the dominant mechanism of change.

To be more specific, consider the rate of change of the H_2 concentration due to reaction 5. At a preignition temperature of about 1200 K, the forward rate $\dot{N}_c$ of reaction 5 is about 10^{-6} moles/cc-s in region 2. With the H_2 and OH concentrations of about 10^{-6} moles/cc and 10^{-12} moles/cc, their chemical time constants τ_{ic} are of the order of 1.0 and 10^{-6}, respectively. This demonstrates clearly that chemistry dominates the evolution of OH. It also implies that prior to ignition, reaction 5 makes a negligible contribution to the rate of change of H_2 and can be neglected with respect to the turbulent mixing rate. With a similar analysis, it can be shown that before-ignition variations in the concentration of all the major species are essentially controlled by turbulence while those of the minor species are controlled by chemistry alone.

By neglecting the chemical evolution of the major species, changes in the bulk properties become decoupled from chemistry for a given propellant. The preignition bulk properties can, thus, be determined only once and then used to investigate the chemical behavior of the minor species in terms of free parameters such as suppressant concentration.

Knowing the bulk properties and neglecting the turbulent mixing term, the conservation equations of the minor species can be reduced to a set of ordinary differential equations with coefficients which depend on the known bulk parameters alone. The behavior of the solution of this set of equations will then determine whether flashing will occur. Figures 6 and 7 show that flashing occurs when the concentration of the minor species O, OH, and H increase monotonically, while Fig. 8 shows that flash is suppressed when there is no such monotonic growth.

4. ALGEBRAIC CRITERION

In this section the algebraic criterion for predicting the onset of muzzle flash is described. It is shown that the criterion is a measure of competing reactions represented by the chain branching reaction 6 and the chain terminating suppressant reaction 18.

To determine an algebraic criterion to predict the onset of muzzle flash, we must determine the conditions which lead to continuous exponential growth of the minor species concentration in region 2. This may be achieved by analyzing the minor species conservation equations along any streamline. Neglecting the turbulent diffusion term, these equations can be written in the general form

$$\frac{dN_i}{dt} + \sum_{j=1}^{\ell} a_{ij} N_j = B_i \quad (i=1,..,m) \tag{3}$$

where ℓ is the total number of species, m is the number of minor species, and along the centerline d/dt=ud/dx. The coefficients a_{ij}, which can be determined from the reactions given in Table 2, are functions of temperature and major or minor species concentrations. The source terms B_i, however, are functions of temperature and only the major species concentration.

The minor species are H, OH, O, K, KO_2, and HO_2. Detailed analysis of the numerical calculation shows that in region 2 the role of potassium atoms is insignificant in the ignition process, and so we neglect it for these considerations. Also from Figures 6-8 we see that the concentration of KO_2 remains basically constant and equal to the original amount of K. Thus, we take KO_2 to be one of the major species with known concentration. Then the minor species to be considered become H, OH, O, and HO_2, which makes m=4 in Equation (3).

Both order of magnitude analysis and numerical calculation show that prior to ignition, the reactions which make significant contribution to the rate of change of the four minor species are reactions 3, 5, 6, 7, 8, 11, 13, 18, 21, 22, 24, 25 in the forward direction and reactions 5, 8 and 24 in reverse direction. In terms of these reactions, the coefficients a_{ij} and B_i become:

$$a_{11} = k_{18}N_9 + k_{11}N_7 + k_6N_7 + f_5N_{12} + f_{24}N_5 \qquad a_{21} = -k_6N_7$$

$$a_{12} = -k_7N_6 \qquad a_{22} = k_7N_6 + f_8N_{12}$$

$$a_{13} = -(k_3N_{10} + k_5N_6) \qquad a_{23} = 0$$

$$a_{14} = B_1 = 0 \qquad a_{24} = B_2 = 0$$

$$a_{31} = -(f_5N_{12} + k_6N_7) \qquad a_{41} = -(k_{11}N_7 + f_{24}N_5)$$

$$a_{32} = -(k_7N_6 + 2f_8N_{12}) \qquad a_{42} = a_{43} = B_4 = 0$$

$$a_{33} = k_3N_{10} + k_5N_6 + k_{21}N_5 \qquad a_{44} = k_{13}N_{10}$$

$$a_{34} = -k_{13}N_{10}$$

$$B_3 = k_{25}N_5N_6$$

where k_r and f_r refer to the r-th reaction forward and reverse rate constants, respectively. N_1, N_2, N_3, N_4, N_5, N_6, N_7, N_9, N_{10}, N_{11}, and N_{12} refer, respectively, to the concentrations of species listed in Table 1.

Since a_{ij} are independent of the 4 minor species concentrations, the set of differential Equation 3 is linear.

THE SOLUTION OF DIFFERENTIAL EQUATIONS

Each of the 4 linear differential equations represenced by Eq. (3) has a homogeneous solution N_{ih} and a particular solution N_{ip} such that

$$\frac{dN_{ip}}{dt} + \sum_j a_{ij} N_{ip} = B_i \tag{4}$$

$$\frac{dN_{ih}}{dt} + \sum_j a_{ij} N_{ih} = 0 \tag{5}$$

The particular solutions are driven by the source term; therefore, variation in N_{ip} must be similar to those of the bulk parameters like temperature. Any exponential growth in the minor species concentrations must then result from the homogeneous solution N_{ih} which can be represented by:

$$N_{ih} = A_i(t)\, e^{\varepsilon(t)t} \quad (i=1,..,4) \tag{6}$$

where $A_i(t)$ and $\varepsilon(t)$ are unknown. Referring to Eq. (2) we note that for the minor species $1/\varepsilon(t)$ must be of the same order of magnitude as τ_{ic}. Differentiating Eq. (6) we get

$$\frac{dN_{ih}}{dt} = A_i \varepsilon e^{\varepsilon t} \left[\frac{\dot{A}}{\varepsilon A_i} + \frac{\dot{\varepsilon}}{\varepsilon} t + 1\right] \tag{7}$$

where $\dot{A} = dA_i/dt$ and $\dot{\varepsilon} = d\varepsilon/dt$. Since the coefficients a_{ij} depend on the bulk properties, then we expect prior to ignition the A_i to be functions of these variables also. Therefore, $\dot{A}_i/A_i$ must be of the order of the turbulent time scale τ_t which implies $\dot{A}_i/\varepsilon A_i \approx \tau_{ic}/\tau_t \ll 1$ and can be neglected with respect to unity. The right-hand side of Eq. (7) can now be equated to $A_i\xi \exp(\varepsilon t)$ where $\xi \equiv d(\varepsilon t)/dt$. Substituting Eq. (7) in Eq. (5) and using the new notation we get:

$$\sum_j A_j (a_{ij} + \xi\delta_{ij}) = 0 \quad (i=1,..,4) \tag{8}$$

where δ_{ij} is a Kronecker delta function.

The unknown coefficients A_j are the solution of Eq. (8). To have a nontrivial solution, however, the determinant of the coefficients must vanish. This requirement results in a 4th order polynomial in ξ which can be written as:

$$\xi^4 + \alpha\xi^3 + \beta\xi^2 + \gamma\xi + \eta = 0 \tag{9}$$

where α, β, γ, and η are functions of a_{ij}. Let σ be a root of Eq. (9); then, using the definition of ξ, we can show that

$$\varepsilon t = \int \sigma dt \tag{10}$$

Referring to Eq. (6) we note that exponentially growing solutions exist when one or more roots of Eq. (9) are positive.

To have a positive root, however, at least one of the coefficients α, β, γ and η must be negative. After considerable algebra it can be shown that in terms of a_{ij} these coefficients are given by:

$$\alpha = a_{11} + a_{22} + a_{33} + a_{44} \tag{11}$$

$$\beta = a_{11}a_{22} + (a_{11} + a_{22})(a_{33} + a_{44}) + a_{33}a_{44} - a_{12}a_{21} - a_{13}a_{31} \tag{12}$$

$$\gamma = (a_{11} + a_{22})a_{33}a_{44} + a_{11}a_{22}(a_{33} + a_{44}) - a_{12}a_{21}(a_{33} + a_{44}) + a_{13}a_{21}a_{32} - a_{13}a_{31}(a_{22} + a_{44}) + a_{13}a_{34}a_{41} \tag{13}$$

$$\eta = a_{44}(a_{11}a_{22}a_{33} - a_{12}a_{21}a_{33} + a_{13}a_{21}a_{32} - a_{13}a_{21}a_{32} - a_{13}a_{31}a_{22}) + a_{13}a_{22}a_{34}a_{41} \tag{14}$$

Using the definitions of a_{ij}, it can be readily shown that both α and β are positive. Hence, according to our formulation, a necessary condition for the onset of muzzle flash is that at least one of the coefficients γ and η be less than zero. By substituting for a_{ij}, it can be shown that to a good approximation these conditions reduce to the relations:

$$2k_6N_7 - (k_{18}N_9 + k_{11}N_7 + f_{24}N_5) > 0 \tag{15}$$

hen $\gamma < 0$, and

$$2k_6N_7 - k_{18}N_9 > 0 \tag{16}$$

when $\eta < 0$. Note that k_6N_7 represents H, OH, and O burning while $k_{18}N_9$ represents suppression by KOH. The significance of the chain branching reaction 6 as the initiator of explosion has been discussed by Dougherty and Rabitz.[13]

At the preignition temperatures of region 2, the term $(k_{11}N_7 + f_{24}N_5)$ makes a significant contribution to the negative term appearing in relation 15. Thus, the inequality 16 will always be satisfied prior to relation 15. We postulate, therefore, that a necessary condition for the onset of muzzle flash is the algebraic criterion given by relation 16. Whether this criterion is also sufficient will be considered in future analyses.

The algebraic criterion can be written in a more convenient form by using the normalized concentration Y_i (Eq. 1), which is basically the same for all the major species. In terms of Y_i the concentrations N_7 (i.e., O_2) and N_9 (i.e., KOH) become:

$$N_7 = 7.29 \times 10^{-3} (1 - Y_7), \qquad N_9 = \frac{X_{09}}{24} Y_9 \tag{17}$$

where 7.29×10^{-3} is the number of moles of O_2 in air per unit mass of air, X_{09} is the mole fraction of KOH at the initial boundary, and 24 is the molecular weight of the propellant. Using the rate constants listed in Table 2 and letting $Y_7 = Y_9 \equiv Y$, the algebraic criterion reduces to the inequality

$$Y < Y^0 \equiv \frac{1.0}{1.0 + 0.214\, \chi_{09} \exp(7250/T)} \tag{18}$$

Y^0 is defined for convenience.

The criterion represented by inequality 18 does not show any direct dependence on such processes as turbulent mixing and KO_2 chemical reactions. These processes may influence the preignition temperature and, thus, have a considerable indirect effect on the criterion. For flows with supersonic initial velocities, typical of those listed in Table 1, higher turbulent mixing rates promote higher frictional heating, hence higher preignition temperatures and higher entrainment rates, hence steeper decline in the axial rates of parameter Y. In the case of higher mixing rates, the combination of these effects is to push the ignition point closer to the initial boundary. The sensitivity of the algebraic criterion on the KO_2 chemical reactions and turbulent mixing rate will be considered in future analysis.

χ_{09}, which is the mole fraction of KOH at the initial boundary, can be related to the fraction of suppressant in the propellant. Therefore, if the preignition temperature is known, the computations used to evaluate χ_{09} are no longer required.

Let B_k be the number of moles of elemental potassium per unit mass of the mixture. In the nonturbulent region upstream of the initial boundary, B_k remains constant along the streamlines. Therefore, at the initial boundary we have:

$$\frac{1}{M} (\chi_{09} + \chi_{013}) = B_k \tag{19}$$

where M is the molecular weight of the propellant gas and χ_{013} is the mole fraction of K species at the initial boundary. Other species containing elemental potassium do not contribute significantly to the left-hand side of

Eq. (19). Referring to Table 1 and Table 3 in Section 5, we note that χ_{013} is an order of magnitude smaller than χ_{09}. Therefore, Eq. (19) yields

$$\chi_{09} \simeq 0.91\ M\ B_k \tag{20}$$

In terms of y_s, the mass fraction of the suppressant in the propellant, B_k is given by:

$$B_k = \frac{a_k}{M_s}\ y_s$$

where M_s is the molecular weight of the suppressant and a_k is the stoichiometric coefficient of elemental potassium in the suppressant. Equation (20) now reduces to:

$$\chi_{09} = 0.91\ a_k\ \left(\frac{M}{M_s}\right)\ y_s \tag{21}$$

For the M30A1 propellant with K_2SO_4 as suppressant, $a_k = 2$, $M_s = 176$ and $M = 24$. With $y_s = 2.5$, 5 and 6, Eq. (21) yields a value of χ_{09} which differs by less than 5 percent from the more exact value listed in Table 1. Since χ_{09} appears linearly in the denominator of Eq. (18), we do not expect the algebraic model to be sensitive to small errors in the value of χ_{09}. Therefore, Eq. (21) can be used to determine the effect of suppressant amount on the flash onset.

Due to the exponential dependence of Y^0 on T (see Eq. (18)), the preignition temperatures must be predicted with reasonable accuracy. The application of the simple criterion would be of no practical value, however, if for each value of χ_{09} the preignition temperatures were to be evaluated numerically. If the preignition temperatures were totally independent of chemistry, then for each propellant the numerical method could be used only once to evaluate the flow temperature assuming frozen chemistry. The

calculated temperature could then be used as the preignition temperature to evaluate Y^0 for any χ_{09}. As shown in Figure 2, however, there is some dependence of preignition temperature on the amount of suppressant and hence chemistry. This is clearly apparent in the difference between the temperatures of the propellants with 5 and 6 percent suppressants. This temperature difference, which is about 10%, may be the result of KO_2 chemistry.

To show the applicability of the simple criterion, we will now assume that the temperature profile of the propellant with 6% suppressant represents the preignitior temperature for all three cases. Since this temperature overlaps the preignition temperature of the propellant with 2.5% suppressant, we expect the predictions of the simple model to be consistent with those of the numerical method for these two cases. This is shown graphically in Figure 9 where Y^0 is plotted versus Y for different values of χ_{09}. (See Eq. 18.) For comparison, Figure 9 also shows the straight line $Y^0 = Y$. According to our formulation, flash is expected if Y^0, given by Eq. (18), intersects the line $Y^0 = Y$. Inspection of Figure 9 shows that as expected the algebraic criterion predicts flash for the propellant with 2.5% suppressant and no flash for the one with 6% suppressant. The failure of the prediction for the 5% case can be explained by referring to Figure 2 which shows the preignition temperature for the 5% case is higher than that of the 6% case which was used to plot Figure 9. Using the value of 1200 K which occurs at the normalized axial distance of about 43 (Figure 2), the calculated result for Y^0 is 0.48 for the propellant with 5% suppressant. At the same station Y has a value less than 0.48. This implies that for this case muzzle flash could have been expected if the correct preignition temperature were used.

The agreement between predictions of the algebraic model and those of the numerical calculation is significant since, given the preignition temperatures, the algebraic model is very simple to apply. The usefulness of the simple model can be greatly enhanced, however, if an equally simple model can be developed to predict the chemical energy release prior to ignition.

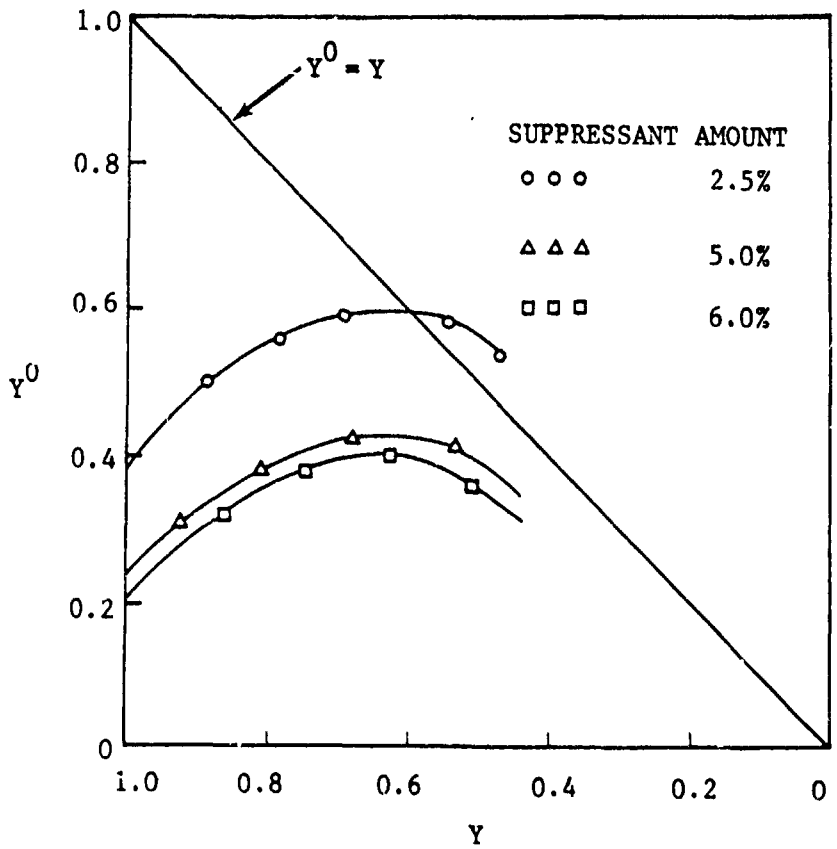

Figure 9. Variation of Y^0 vs. Y for Three Different Values of X_{09}, the Amount of Suppressant.

A significant feature of the algebraic model is that it displays the parameters which are most important to the onset of muzzle flash. These are the suppressant amount and the forward rate constants of reactions 6 and 18. Through its dependence on preignition temperature, the criterion also displays, indirectly, the possible effects of KO_2 chemical reaction and the effect of turbulent mixing rate. These comprise a considerably smaller set of parameters for characterizing the ignition process than the total number one may derive from the number of species and reactions given in Tables 1 and 2.

It should be emphasized here that the algebraic criterion is valid for the set of rate constants listed in Table 2. The formulation leading to the algebraic criterion must be repeated when the rate constants describing the chemistry of the minor species are changed. This is necessary in order to determine if the nonlinear terms, which were neglected in Eq. (3), become important. If the nonlinear terms become important, a different method of solution may be required.

5. FURTHER VALIDATION OF THE MEFF MODEL

During the development of the MEFF model, an 8-inch gun utilizing three different propellants, designated M30A1, M30A2, and M31E1, was used to test the model and demonstrate its validity. For these three cases the model flash/no-flash predictions were consistent with observation.

To further validate the MEFF model, the observed flash/no-flash of five additional gun systems was compared to that of the model predictions. A description of the five new cases is given below.

- Case 1 is an 81 mm mortar whose propellant contains no flash suppressant. It was observed to flash every time it was fired.
- Case 2 is an 81 mm mortar containing 2.0% flash suppressant in its propellant. No flash has been observed from the firing of this mortar.
- Case 3 is a 155 mm howitzer with a standard M203 charge having 4.6% suppressant. An observation has shown no flash.
- Case 4 is the same 155 mm howitzer with 0.36 Kg (about 3%) of the M203 propellant removed. Several observations have shown flash.
- Case 5 is a 155 mm howitzer with reduced M4A2 charge containing 1% suppressant. Flash has been observed with each firing.

To predict the muzzle flash onset for these five cases, the procedures described in Reference 3 were used to determine the input variables required to exercise the MEFF model. The resulting input variables are listed in Table 3. The initial conditions refer to the parameters at the initial boundary of the afterburning region.

Table 3. Calculated Mixing Region Boundary Conditions For Five New Gun Systems

Case Number	1	2	3	4	5
Percent Suppressant	0.0	2.0	4.6	4.6	1.0
Mixing Region Boundary T(K)	918	901	984	989	991
Mixing Region Boundary P(Atm)	1.0	1.0	1.0	1.0	1.0
Mixing Region Boundary U(m/sec)	1845	1815	1924	1921	1722
Mixing Region Boundary Mole Fraction					
H	3.133(-5)	2.296(-5)	7.123(-5)	7.231(-5)	2.049(-5)
O	1.365(-9)	7.292(-10)	1.874(-8)	1.906(-8)	2.028(-10)
OH	2.960(-6)	2.058(-6)	1.002(-5)	1.020(-5)	8.042(-7)
HO_2	1.000(-12)	1.000(-12)	1.000(-12)	1.000(-12)	1.000(-12)
KO_2	0.000	1.000(-12)	1.000(-12)	1.000(-12)	1.000(-12)
H_2	1.433(-1)	1.382(-1)	1.368(-1)	1.365(-1)	2.178(-1)
O_2	8.075(-10)	4.471(-10)	1.377(-8)	1.410(-8)	6.823(-11)
N_2	1.129(-1)	1.156(-1)	2.821(-1)	2.821(-1)	2.744(-1)
KOH	0.000	4.780(-3)	1.077(-2)	1.089(-2)	2.040(-3)
CO	4.032(-1)	3.948(-1)	2.422(-1)	2.427(-1)	2.824(-1)
CO_2	1.371(-1)	1.435(-1)	1.010(-1)	1.005(-1)	6.160(-2)
H_2O	2.035(-1)	2.025(-1)	2.255(-1)	2.258(-1)	1.614(-1)
K	0.000	5.813(-4)	1.530(-3)	1.545(-3)	4.091(-4)

The results of flash prediction are shown in Figure 10, where for each axial station X/R (R is the initial boundary radius), the maximum plume gas temperature over plane cross sections normal to the X axis is plotted versus X/R. Note that during the initial development of the plume, the maximum plume temperature does not necessarily occur along the same radial distance (e.g., the plume center line). Therefore, it is more informative to show the maximum temperature in planes normal to a given axial station.

In the MEFF model flash is indicated by a sudden jump in the plume temperature. As Figure 10 shows the model predicts muzzle flash onset for cases 1 and 5 and no-flash for cases 2, 3, and 4. Except for case 4 the predictions are consistent with observation.

The problem with case 4 is explained by noting that cases 3 and 4 are the same except for a 3% difference in their propellant mass. The fact that such a small difference results in different observed flash/no-flash outcome indicates that case 3 or 4 is a borderline case. In such cases variations in parameters such as ambient conditions (wind, temperature, humidity, etc.) which are not included in the MEFF model may play a decisive role in the outcome of observation.

Figure 10 shows nearly identical computed temperature profiles for cases 3 and 4; yet the observations show flash for case 4 and no-flash for case 3. We infer that these two cases, with a 3% difference between the amount of their charge, indicate the degree of sensitivity of the MEFF model as presently developed and executed. Simply put, this model is not yet able to distinguish this small a change. Because of errors inherent in the model input data, there will always exist a region of output predictions that will be uncertain. Answers falling within this region that turn out to be correct must be judged fortuitous.

What seems peculiar to borderline cases is the fact that the predicted maximum plume temperature continues to increase over considerably longer distances than those of the nonborderline propellant. In such cases the

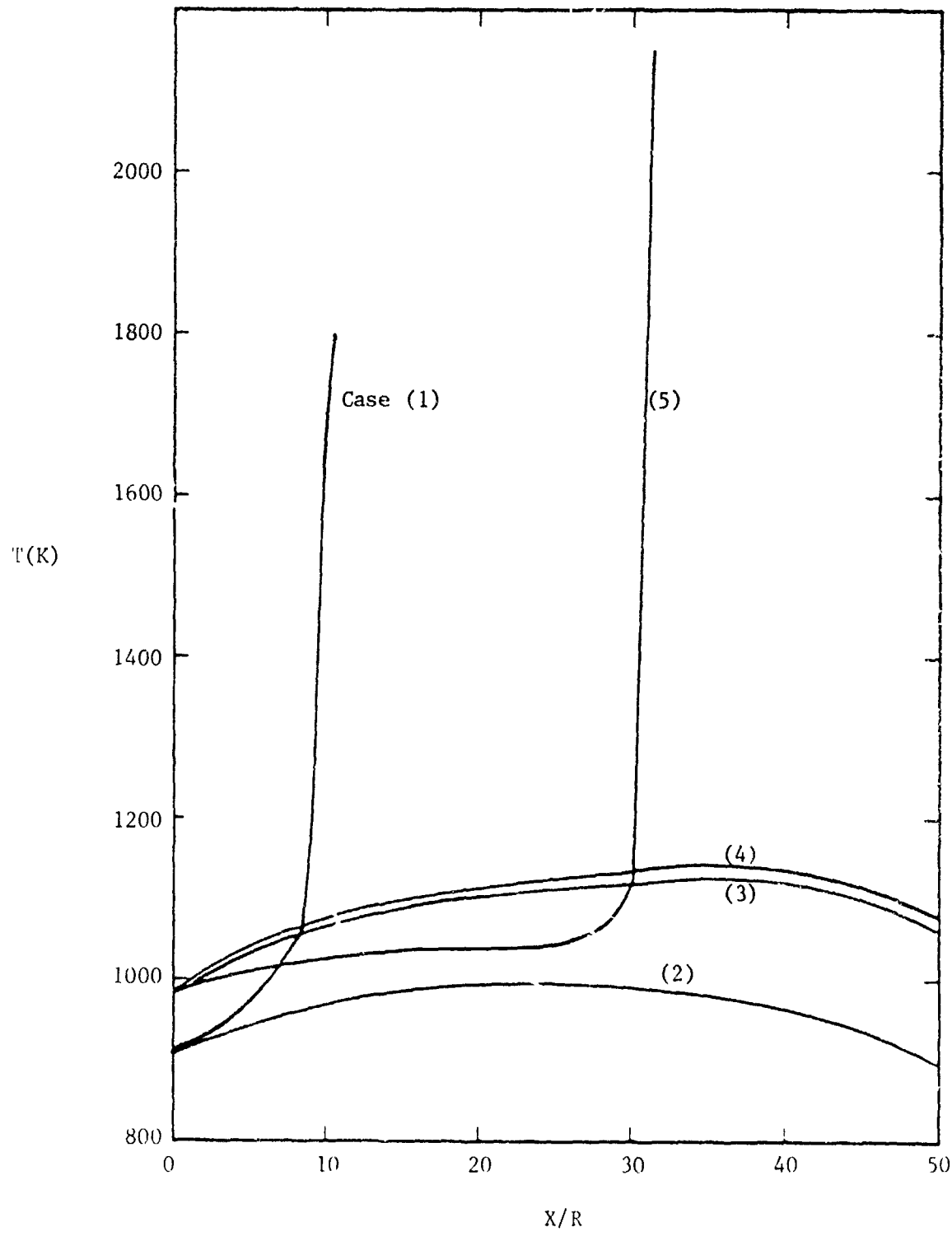

Figure 10. Predicted Maximum Axial Plane Temperature Versus Distance for Cases 1 Through 5.

calculation must be continued far downstream before it can be determined for certainty if flash is predicted.

Although additional comparison with observation may be required to fully validate the predictive accuracy of the MEFF model, the fact that the model is "consistent" with observations for several different cases is encouraging, considering the complexity of the phenomenon which has been modeled.

Comparison of the Algebraic and MEFF Predictions

We now compare the predictions of the algebraic model, given by Eq. (16), with those of the MEFF model. We will not use Eq. (18) since it is an approximate form of Eq. (16). For the convenience of presentation, we first rewrite the relation (16) in the following form

$$2k_6N_7 \left[1 - \frac{k_{18}}{2k_6} \frac{\chi_9}{\chi_7}\right] > 0 \qquad (22)$$

where χ_9 and χ_7 are the mole fraction of KOH and O_2, respectively. Let F represent the term in the square brackets. Since the product $2k_6N_7$ is positive, then the algebraic criterion can also be represented by:

$$F = 1 - 3.75 \times 10^{-2} \exp(7250/T) \frac{\chi_9}{\chi_7} > 0 \qquad (23)$$

we have used the rate constants listed in Table 2 to replace k_{18} and k_6.

Given T, χ_9 and χ_7 along any streamline, F can be plotted vs the axial direction X/R. If at any point F becomes greater than zero, we expect the onset of muzzle flash. This is because positive F indicates the exponential growth of the minor species H, O, and OH. For cases 2, 4, and 5 this is shown in Figure 11. Case 1 is not considered since it does not contain any

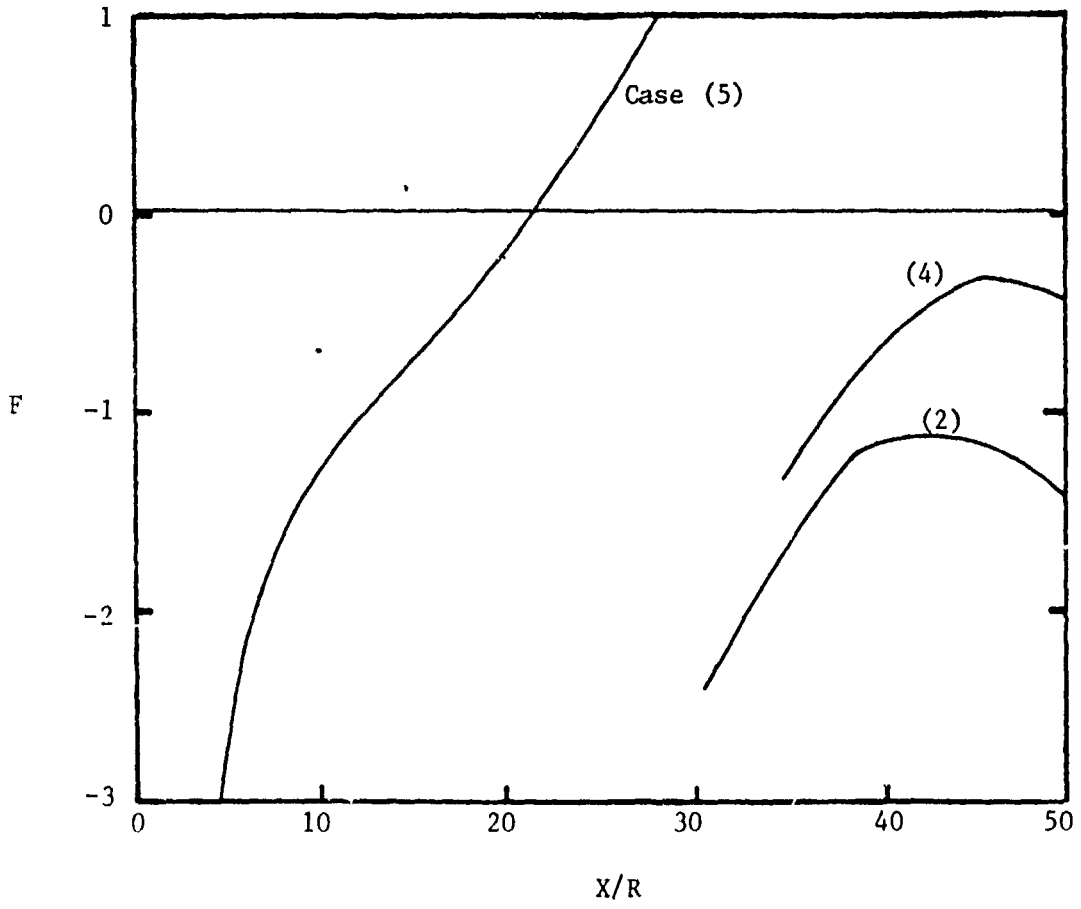

Figure 11. Variation of Function F Versus Distance for Cases 2, 4, and 5.

suppressant and hence Eq. 23 does not apply to it. Case 3 is not included since it is basically the same as case 4.

To obtain Figure 11 we have used the computed results of the MEFF model. The flowfield points on Figure 11 correspond to those shown in Figure 10, at which the temperature is a maximum. For cases 2 and 4 the portion of the graph where the function F attains its maximum value is shown.

As shown in Figure 11, for case 5 the function F becomes greater than zero at $X/R \simeq 22$; therefore, we expect the predicted flash to occur downstream of this point. This is confirmed by referring to Figure 10 which shows that case 5 flashes at $X/R \simeq 31$. For cases 2 and 4 the function F is always negative; therefore, consistent with Figure 10, no flash is expected. Note, however, that for case 4, which is a borderline case, F is considerably closer to crossing the zero point than for the nonborderline propellant case 2.

We conclude, therefore, that the predictions of the algebraic model are consistent with those of the MEFF model.

6. PARAMETRIC ANALYSIS

The development of a mathematically tractable model describing a complicated phenomenon, such as muzzle exhaust flowfield, requires considerable simplifying assumptions. These assumptions, however, may generate high levels of uncertainties in the calculated results. For turbulent and chemically reacting flows, there are the additional sources of uncertainty related to the experimentally measured chemical rate constants and the turbulent mixing models. The objective of this section is to vary the muzzle, chemical, and turbulent mixing parameters with respect to their nominal values in order to determine an uncertainty range within which the predicted results become insensitive to variations in these parameters. This type of analysis can lead the future model improvements towards those phenomena which are most sensitive to variation in such parameters.

A similar senstivity analysis was performed during our previous effort and reported in Reference 3. Based on the previous sensitivity analysis, the more realistic chemical reaction set shown in Table 2 was selected as the "baseline" kinetics set. The baseline parameters for the three propellants considered here are listed in Table 4. As in our previous analysis, the three propellants considered in this sensitivity analysis are M30A1, M30A2, and M31E1. Note that the initial boundary conditions for these baseline propellants are different from their corresponding values reported in Reference 3. This is due to the changes made in the size of the normal shock as suggested by Schmidt[7] (Section 2). Using the baseline conditions, the MEFF model predicts the onset of muzzle flash for the M30A1 and M30A2 propellants and no flash for the M31E1 propellant. All of these predicted results are consistent with observation.[2]

Table 4. Calculated Initial Boundary Conditions for The Baseline Propellants

Propellant	M30A1	M30A2	M31E1
Percent Suppressant	1% K_2SO_4	2.7% KNO_3	1% K_2SO_4
Mixing Region Boundary T(K)	1018	1030	840
Mixing Region Boundary P(atm)	1	1	1
Mixing Region Boundary U(m/sec)	1888	1886	1757
Mixing Region Boundary Mole Fraction			
H	7.031(-5)	8.013(-5)	5.645(-6)
O	1.396(-8)	2.118(-8)	1.643(-11)
OH	8.727(-6)	1.114(-5)	1.576(-7)
HO_2	1.000(-12)	1.000(-12)	1.000(-12)
KO_2	1.000(-12)	1.000(-12)	1.000(-12)
H_2	1.500(-1)	1.434(-1)	2.077(-1)
O_2	9.320(-9)	1.516(-8)	6.010(-12)
N_2	2.782(-1)	2.772(-1)	2.907(-1)
KOH	2.460(-3)	5.364(-3)	2.113(-3)
CO	2.515(-1)	2.494(-1)	2.630(-1)
CO_2	9.410(-2)	9.709(-2)	7.500(-2)
H_2O	2.233(-1)	2.266(-1)	1.612(-1)
K	3.725(-4)	8.213(-4)	2.772(-4)

Sensitivity with Respect to Muzzle Conditions

The first parameter considered for analysis is the average barrel gas temperature which is calculated using the method of Baer and Frankle.[14] The average temperature is used to determine the muzzle pressure and temperature and hence the afterburning region initial conditions. To the best of the author's knowledge, the accuracy of the muzzle temperature determined by this procedure has not yet been verified by measurements. Hence, a sensitivity analysis is only meaningful in the sense that it indicates how inaccurate the measured values may be before model improvements are necessary.

An increase in the muzzle temperature increases the temperature and the velocity of the propellant gas at the mixing region boundary. This causes the temperature in the preignition region to increase as a result of higher initial temperatures and additional heating due to a higher rate of mixing. Since some of the important chemical rate constants are exponential functions of temperature, one can expect relatively small changes in the muzzle temperature and pressure to cause significant changes in the outcome of the predictions. The species concentration can also change as a result of changes in the conditions at the muzzle and the rates of mixing; these changes, however, are not as significant.

For the three baseline propellants considered, Table 5 shows the sensitivity of the predicted muzzle flash onset in terms of variations in T_{av}, the calculated average barrel gas temperature. For comparison, baseline results are also shown together with T_i, the afterburning region initial temperature. A temperature interval of 100 K is chosen. It is hoped that within ±100 K the calculated T_{av} equals the actual T_{av}. Table 5 shows that for the baseline cases the predicted results are not sensitive to variations of ±100 K in the calculated T_{av}. When T_{av} is changed by 200 K, all three cases, however, yield results different from those of the baseline predictions. Thus, these predictions of the MEFF model are not sensitive to calculated valued of (T_{av} ± 100 K).

Table 5. Dependence of Predicted Flash Onset on Calculated Average Barrel Gas Temperature

Propellant Type	Predicted Flash Onset				
	T_{av} - 200 K	T_{av} - 100 K	Baseline	T_{av} + 100 K	T_{av} + 200K
M30A1	No Flash (T_i = 922 K)*	Flash (T_i = 971 K)	Flash (T_i = 1018 K)	-	-
M30A2	No Flash	Flash (T_i = 982 K)	Flash (T_i = 1030 K)	-	-
M31E1	-	-	No Flash (T_i = 840 K)	No Flash (T_i = 886 K)	Flash (T_i = 932 K)

*T_i is the mixing region boundary temperature.

The analysis described in Ref. 3 showed somewhat more sensitive dependence of the predicted flash onset on variation in T_{av}. The difference is due to both changes in the initial conditions, as described in Section 2, and the addition of the KO_2 and HO_2 chemistry in the chemical kinetics set.

Sensitivity with Respect to Turbulent Mixing Rate

The turbulent mixing rate controls the O_2 entrainment rate into the plume and the level of plume viscous heating. Both of these can affect the onset of muzzle flash. Several eddy diffusivity models are available in the computational method described in LAPP.[6] The one considered in the MEFF is the Donaldson-Gray[6] model which is appropriate for jets with supersonic initial velocities. The eddy viscosity models generally contain an arbitrary constant, the value of which is fixed to reproduce turbulent flows with known properties. The value listed in Ref. 6 is used in our baseline calculations. The sensitivity of the predicted flash onset for the M30A1, M30A2, and M31E1 propellants with respect to variations in the nominal value of the mixing rate coefficient, denoted here by α, is now considered.

The nominal value of α is 1. A reduction in α lowers the entrainment rate of O_2. Therefore, for M30A1 propellant we expect smaller α to result in either a time delay in the ignition or possibly total flash inhibition. This is tested here by decreasing α by a factor of 5. The result is shown in Figure 12 where the plume maximum temperature in the plane normal to X/R is plotted vs X/R and α. As shown in Figure 12 the result of reducing α is a delay in the ignition point. An increase in α is expected to have the opposite effect. For the M30A1 propellant this is also shown in Figure 12 which indicates that increasing α by a factor of 5 results in earlier predicted flashing. Since we do not expect the nominal value of α to be in error by more than a factor of 5, we conclude that for the M30A1 case the onset of muzzle flash is independent of α.

The sensitivity of the M30A2 propellant with respect to α is also shown in Figure 12. As in the M30A1 propellant, reducing α by a factor of 5 only

delays the predicted flash onset, while increasing α by a factor of 2.5 leads to earlier predicted flashing for the M30A2 propellant. Unlike the M30A1 propellant, however, increasing α by a factor of 5 results in a predicted suppressed flash. This can be explained by noting that increasing α leads to both enhanced frictional heating and, as a result of mixing with colder atmosphere, increased rate of cooling. In the supersonic flow regions the net effect is higher temperatures, while in the subsonic regions the net effect is lower temperatures with respect to α=1 case. The result as seen in Figure 12 is a narrow high temperature flow region which is shifted towards the muzzle. The absence of the muzzle flash implies that either the reacting gas resident time in this high temperature region is short compared to the ignition induction time or the enhanced mixing generates a propellant-air mixture ratio whose ignition temperature is greater than the plume temperature.

The M30A1 propellant contains half as much suppressant as the M30A2 propellant. Therefore, for the same propellant-air mixture, the M30A1 has lower ignition temperature, causing it to ignite earlier when α is increased by a factor of 5. We expect the M30A1 propellant would be suppressed for sufficiently high values of α.

We conclude, therefore, that the M30A2 propellant is more sensitive to variations in α than the M30A1 propellant. Observation has shown that the M30A2 propellant flashes occasionally. Therefore, the higher sensitivity with respect to parameters such as α may be attributed to the fact that the M30A2 propellant is a borderline case.

The sensitivity of the M31E1 propellant with respect to α is also shown in Figure 12. For this case no muzzle flash was predicted when α varied by a factor of 5. For the sake of clarity, the α=0.5 rather than the α=0.2 case (which has a much lower rate of friction induced temperature rise) is shown in Figure 12.

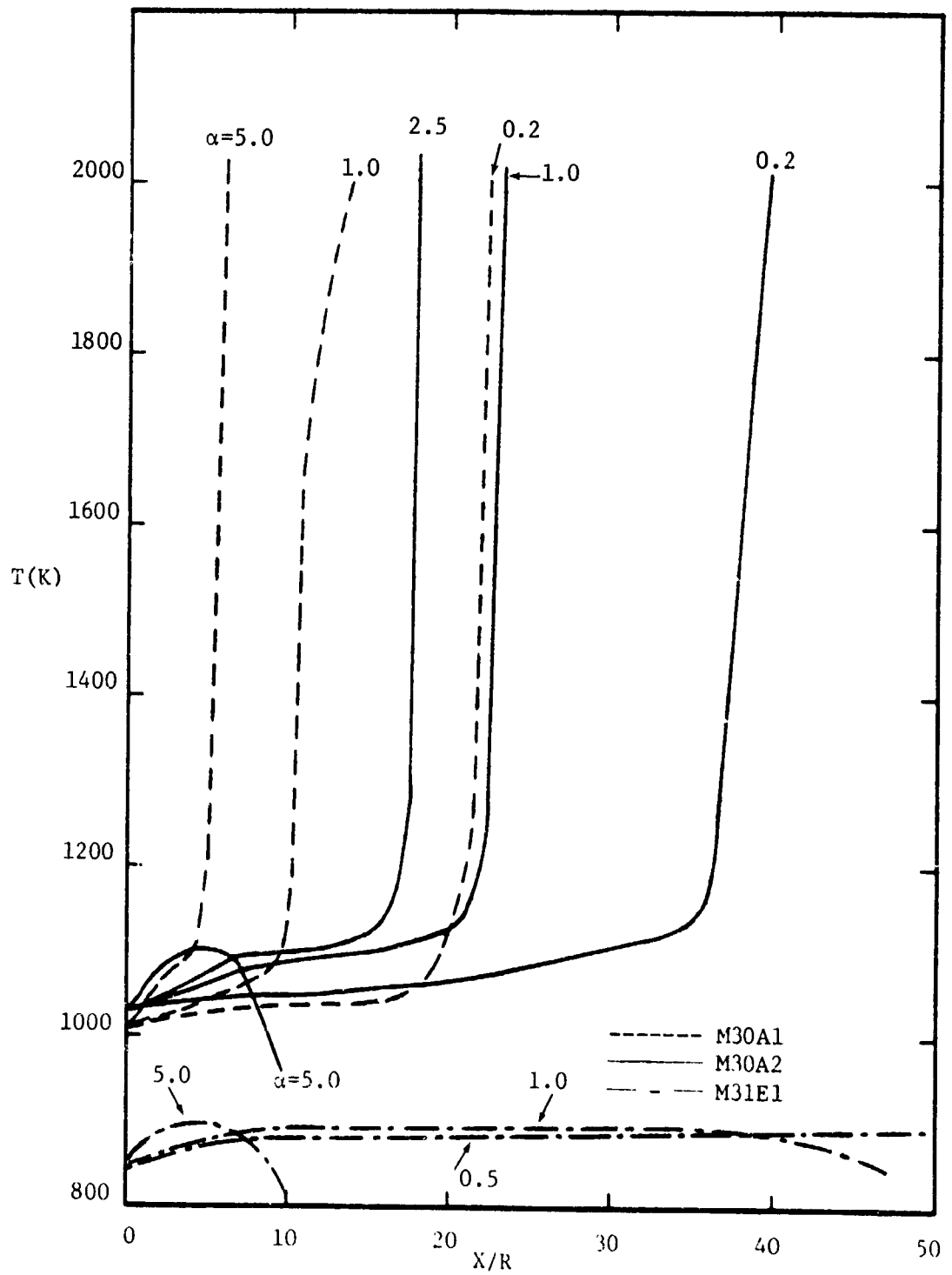

Figure 12. Predicted Maximum Axial Plane Temperature Versus Distance and α for M30A1, M30A2, and M31E1 propellants.

Sensitivity With Respect to Chemical Rate Constants

As shown in Table 2, there is a considerable range of uncertainty in the reported rate constants used in our analysis. Most of the largest uncertainties, however, are associated with 3-body reactions (e.g., reactions Number 5,10,13) which are not significant during the preignition period.

The forward rates associated with the above mentioned 3-body reaction are proportional to the concentration of species like H, O, and OH, whose initial concentration is insignificant. Therefore, unless the amount of these species increases significantly, these 3-body reactions will play no important role. As shown in Section 3, ignition occurs when the concentration of species, such as H, grow exponentially. Due to the rapid concentration growth in the concentration of H, O, OH species, the uncertainty factors of 30 in their rate constants will have little effect on the eventual effectiveness of these 3-body reactions.

In Section 3, we showed that in the preignition region, only a few reactions determine if muzzle flash will occur. Of those reactions, those that involve potassium containing species are the most important in the theoretical analysis of muzzle flash suppression. These are Reactions 18,19,21,22,24, and 25 of Table 2. Due to the small initial concentrations of OH, the role of the 3-body Reaction 19 is negligible in the preignition region. Of the remaining reactions the rates of those containing KO_2 species are the most uncertain.

The sources of uncertainty in a reaction involving KO_2 are twofold: the uncertainty in the measured or estimated forward rate coefficient and the uncertainty in the heat of formation of KO_2. This quantity is needed to evaluate the equilibrium constant for the reaction and so determine the reverse rate constant. The heat of formation can be obtained from the more easily measured dissociation energy. Computer experiments have shown that a dissociation energy of 55 cal/mole (value used in our original calculations reported in Ref. 3) makes the backward rate of Reaction 21 so fast that it becomes both a significant sink for KOH and a source for OH.

Large reductions in the concentration of KOH can reduce the effectiveness of the main suppressant Reaction 18 and hence enhance the chances of a flash prediction.

As discussed in Section 3, we have assumed the dissociation energy of KO_2 is the same as that of NaO_2 and equal to 36 kcal/mole. This reduction of about 20 kcal/mole makes all the predicted results consistent with observations.

Due to the strong dependence of the predictions on the variations in the KO_2 dissociation energy, any sensitivity analysis based only on the uncertainties in the rate constants of reactions containing KO_2 is inconclusive. Such sensitivity analysis will be meaningful when measured KO_2 dissociation energies become available. Recently, Figger et al [15] have reported a measured value of about 45 kcal/mole for the dissociation energy of KO_2. Currently, measurements are being conducted at Aerodyne Research, Inc., to determine not only the KO_2 dissociation energy but also the forward rate constants of some of the important reactions containing the KO_2 species. Once these measurements are completed, a full sensitivity analysis in terms of suppressant reaction rate constants could be undertaken.

The only reaction involving potassium containing species which are least effected by the KO_2 thermodynamic data are: Reaction 18, which is independent of KO_2 data, and Reaction 22, which in the preignition region proceeds practically in the forward direction alone. The rate of Reaction 22 is proportional to the product of its rate constant and the concentration of O_2. As a result of turbulent entrainment, the concentration of O_2, which is negligible at the initial boundary, increases by several orders of magnitude in the preignition region. Therefore, variations by a factor of 10, the uncertainty factor of Reaction 22 rate constant, will have insignificant effects on the forward rate of Reaction 22 which converts K into KO_2. (See Section 3.) This was demonstrated for M30A1 propellant. A factor of 5 reduction in the rate constant of Reaction 22 resulted in a short delay in the ignition point.

The sensitivity of the predicted results with uncertainties in the forward rate constant of the suppressant Reaction 18 is, therefore, the only meaningful analysis at the current level of chemical model development. For this objective, we consider the baseline propellants, M31E1, M30A1, and M30A2.

For the cool-burning M31E1 propellant, the MEFF model did not predict the onset of muzzle flash even in the absence of suppressant. For cool-burning propellants, the 3-body Reaction 11, which converts H into HO_2, plays a role similar to that of suppressant Reaction 18. Therefore, for M31E1 propellant, sensitivity analysis with respect to Reaction 18 is not required.

In the absence of suppressant, the M30A1 and M30A2 propellants are practically identical. There are, however, about twice as many moles of potassium in the M30A2 propellant, which contains 2.7 % KNO_3, than in the M30A1 propellant, which contains 1.0 % K_2SO_4. This results in the small differences in the initial conditions of the M30A1 and M30A2 propellants as listed in Table 4. The MEFF model predicts the onset of muzzle flash for both of these propellants. The increased amount of potassium in the M30A2 propellant, however, delays the ignition point.

The rate of Reaction 18 is proportional to the product of its forward rate constant and the concentration of KOH. Therefore, an increase in the rate for this reaction is equivalent to an increase in the concentration of KOH or vice versa. Hence, to determine the sensitivity of the predictions with respect to the rate constant of Reaction 18, it is sufficient to consider in detail the M30A1 propellant alone.

The MEFF model predictions show that increasing the forward rate constant of Reaction 18 by factor of 2 and 4 only causes a delay in the predicted ignition point of muzzle flash for the M30A1 propellant. An increase by a factor of 6 and higher, however, results in a predicted suppressed flash. This implies that within the uncertainty limits listed in Table 2, the MEFF prediction for the M30A1 propellant are not sensitive to variations in the

forward rate constant of Reaction 18. The reported uncertainty factor of Reaction 18 rate constant, however, is valid only for the temperature range 1800 to 2200 K. The uncertainty factor may be higher outside this temperature range.

Having more suppressant, the M30A2 propellant is expected to be more sensitive to variations in the rate constant of Reaction 18. The MEFF model shows that increasing the rate constant of Reaction 18 by a factor of only 4 causes the M30A2 propellant not to flash.

7. CONCLUSIONS AND RECOMMENDATIONS

CONCLUSIONS

In this report we have developed an algebraic criterion to predict the onset of muzzle flash. The formulation leading to the criterion is based on the results of more accurate numerical calculations which consider turbulent mixing and detailed chemical kinetics.

For several propellant formulations considered, the predictions of the algebraic criterion were consistent with those of the numerical calculations. This agreement is significant since the criterion can be considerably simpler to apply than the numerical method.

The algebraic model requires the preignition flow temperature which depends on the mixing properties and chemistry. The usefulness of the criterion may be greatly enhanced if simple models accounting for the chemical heat release in the preignition region can be developed.

The numerical muzzle exhaust flow field (MEFF) model was used to predict the muzzle flash onset for several gun systems. Except for a borderline case, the flash onset predictions were in agreement with observation. This result further validates the MEFF model.

The sensitivity of the model predictions with respect to variations in such key parameters as muzzle temperature, suppressant reaction (Reaction 18 of Table 2) rate constant, and turbulent mixing rate were also considered. For the three baseline propellants, the analysis suggests that: (a) For non-borderline propellant, the flash onset prediction is independent of variations by a factor of at least 5 in the turbulent mixing rate. (b) The predicted flash onset is insensitive to variations of ± 100K in the average barrel gas temperature. (c) The sensitivity of the predicted flash onset with respect

to suppressant reaction rate constant varies with propellant type. The MEFF code predicts a no-flash condition for the cool-burning M31E1 propellant, even in the absence of suppressant. Therefore, the M31E1 propellant is independent of suppressant chemistry. The flash onset prediction for M30A1 propellant is insensitive to variations within a factor of 6 in the suppressant reaction rate constant. The M30A2 propellant, which has twice as much suppressant as M30A1, is insensitive to variations within a factor of 4 in the suppressant reaction rate constant.

While more data comparison and sensitivity analysis with respect to other important variables (e.g., KO_2 thermodynamic data) are required to probe the limits of both the numerical model and the algebraic criterion, we believe that both models are a reasonable first approach for analyzing a complicated phenomenon such as muzzle exhaust flow field.

RECOMMENDATIONS

To enhance the reliability of the muzzle exhaust flow field developed here, the following additional analyses are recommended:

- Sensitivity Analysis
  - Determine the sensitivity of the model predictions with respect to variations in the KO_2 dissociation energy and variations in the rate constants of those chemical reactions which contain KO_2. (See Table 2.)
- Analytical Improvements
  - Improve the current model by including the barrel and reflected shock heating and including the flow nonuniformities in the afterburning region boundary condition. These improvements may increase the reliability of the model when predicting the flash for marginally suppressed propellants.

- To assess the effects of flow nonsteadiness on flash onset, develop a nonsteady reacting and mixing flow model using the relatively simple plume models to describe the motion of the afterburning flow fields. This will also yield an estimate of the plume penetration distance in the atmosphere.
- Using the experience gained from the analysis of the simpler nonsteady model, which may isolate the time and length scales important for flash prediction, develop a more sophisticated numerical method of predicting the flow field of an axisymmetric, nonsteady, turbulent, and chemically reacting plume.

ACKNOWLEDGEMENTS

The author wishes to express his gratitude to Drs. J.C. Wormhoudt, C.E. Kolb and A. Freedman of Aerodyne and Drs. I.W. May and J.M. Heimerl of Army Ballistic Research Laboratory for many useful discussions.

This work was sponsored by U.S. Army Ballistic Research Laboratory under Contract No. DAK11-81-Q-0074.

REFERENCES

1. S.P. Carfagno, Handbook on Gun Flash, The Franklin Institute, Contract No. DA-36-034-501-ORD-78RD, Nov. 1961 (AD 327051).

2. I.W. May and S.I. Einstein, "Prediction of Gun Muzzle Flash," Ballistic Research Laboratory Technical Report ARBRL-TR-02229, Aberdeen Proving Ground, Maryland, March 1980 (ADA 083888).

3. V. Yousefian "Muzzle Flash Onset," Aerodyne Research, Inc., 45 Manning Road, Billerica, MA, ARI-RR-236, November 1980.

4. V. Yousefian, I.W. May, and J.M. Heimerl, "Modeling the Occurrence of Muzzle Flash in Guns," 17th JANNAF Combustion Meeting, CPIA Publication 329, November 1980.

5. D.E. Jensen and G.A. Jones, "Reaction Rate Coefficients for Flame Calculations," Combustion and Flame, 32, 1978.

6. R.R. Mikatarian, C.J. Kau, and H.S. Pergament, "A Fast Computer Program for Nonequilibrium Rocket Plume Prediction," Air Force Rocket Propulsion Laboratory, Report No. AFRPL-TR-72-94.

7. E.M. Schmidt, "Gun Muzzle Flash and Associated Pressure Disturbances," AIAA 16th Thermophysics Conference, AIAA-81-1109 (1981).

8. D.E. Jensen and G.A. Jones, Combustion and Flame, 41, 71-85 (1981).

9. JANAF Thermochemical Tables, Dow Chemical Company, Midland (continuously updated).

10. C.J. Howard, J. Amer. Chem. Soc., 102, 6937 (1980).

11. C.J. Dougherty, M.J. McEwan, and I.E. Phillips, Combustion and Flame, 21, 253 (1973).

12. M.H. Alexander, J. Chem. Phys., 69, 3502 (1978).

13. E.P. Dougherty and H. Rabitz, J. Chem. Phys, 72, 6571 (1980).

14. P. G. Baer and J. M Frankle, "The Simulation of Interior Ballistic Performance of Guns by Digital Computer Program," Ballistic Research Laboratories Report No. 1183, Aberdeen Proving Ground, Maryland, Dec. 1962 (AD 29980).

15. H. Figger, A. Kowalski, X.H. Zhu, "Chemiluminescent Reaction Between Alkali Dimers and Oxygen Molecules," 50 Years Dynamics of Chemical Reactions Deutsche Bunsengesellschaft für Phys. Chemie, Hahn-Meitner-Institut für Kernforschung, Berlin, Gmbh, HMI-B362 October 1981.

DISTRIBUTION LIST

No. Of Copies	Organization
12	Administrator Defense Technical Info Center ATTN: DTIC-DDA Cameron Station Alexandria, VA 22314
1	Office of the Under Secretary of Defense Research & Engineering ATTN: R. Thorkildsen Washington, DC 20301
1	HQDA/SAUS-OR, D. Hardison Washington, DC 20301
1	HQDA/DAMA-ZA Washington, DC 20310
2	HQDA, DAMA-CSM, A. German E. Lippi Washington, DC 20310
1	HQDA/SARDA Washington, DC 20310
1	Commandant US Army War College ATTN: Library-FF229 Carlisle Barracks, PA 17013
1	Ballistic Missile Defense Advanced Technology Center P. O. Box 1500 Huntsville, AL 35804
1	Chairman DOD Explosives Safety Board Room 856-C Hoffman Bldg. 1 2461 Eisenhower Avenue Alexandria, VA 22331
3	Commander US Army Materiel Development and Readiness Command ATTN: DRCDMD-ST DCRSF-E, Safety Office DRCDE-DW 5001 Eisenhower Avenue Alexandria, VA 22333
14	Commander US Army Armament R&D Command ATTN: DRDAR-TSS DRDAR-TDC D. Gyorog DRDAR-LCA K. Russell A. Moss J. Lannon A. Beardell D. Downs S. Einstein L. Schlosberg S. Westley S. Bernstein P. Kemmey C. Heyman Dover, NJ 07801
9	US Army Armament R&D Command ATTN: DRDAR-SCA, L. Stiefel B. Brodman DRDAR-LCB-I, D. Spring DRDAR-LCE, R. Walker DRDAR-LCU-CT E. Barrieres R. Davitt DRDAR-LCU-CV C.Mandala E. Moore DRDAR-LCM-E S. Kaplowitz Dover, NJ 07801

DISTRIBUTION LIST

No. Of Copies	Organization
5	Commander US Army Armament R&D Command ATTN: DRDAR-QAR, J. Rutkowski Dover, NJ 07801
7	Project Manager Cannon Artillery Weapons System ATTN: DRCPM-CAWS F. Menke (3 cys) DRCPM-CAWS-WS H. Noble DRCPM-CAWS-SI M. Fisette DRCPM-CAWS-AM R. DeKleine H. Hassmann Dover, NJ 07801
3	Project Manager Munitions Production Base Modernization and Expansion ATTN: DRCPM-PMB, J. Ziegler M. Lohr A. Siklosi Dover, NJ 07801
3	Project Manager Tank Main Armament System ATTN: DRCPM-TMA, D. Appling DRCPM-TMA-105 DRCPM-TMA-120 Dover, NJ 07801
4	Commander US Army Armament R&D Command ATTN: DRDAR-LCW-A M.Salsbury DRDAR-LCS DRDAR-LCU, A. Moss DRDAR-LC, I. Frasier Dover, NJ 07801
5	Commander US Army Armament Materiel Readiness Command ATTN: DRSAR-LEP-L DRSAR-LC, L. Ambrosini DRSAR-IRC, G. Cowan DRSAR-LEM, W. Fortune, R. Zastrow Rock Island, IL 61299
1	Commander US Army Watervliet Arsenal ATTN: SARWV-RD, R. Thierry Watervliet, NY 12189
1	Director US Army ARRADCOM Benet Weapons Laboratory ATTN: DRDAR-LCB-TL Watervliet, NY 12189
1	Commander US Army Aviation Research and Development Command ATTN: DRDAV-E 4300 Goodfellow Blvd. St. Louis, MO 63120
1	Commander US Army TSARCOM 4300 Goodfellow Blvd. St. Louis, MO 63120
1	Director US Army Air Mobility Research And Development Laboratory Ames Research Center Moffett Field, CA 94035

DISTRIBUTION LIST

No. Of Copies	Organization
1	Commander US Army Communications Research and Development Command ATTN: DRDCO-PPA-SA Fort Monmouth, NJ 07703
1	Commander US Army Electronics Research and Development Command Technical Support Activity ATTN: DELSD-L Fort Monmouth, NJ 07703
1	Commander US Army Harry Diamond Lab. ATTN: DELHD-TA-L 2800 Powder Mill Road Adelphi, MD 20783
2	Commander US Army Missile Command ATTN: DRSMI-R DRSMI-YDL Redstone Arsenal, AL 35898
1	Commander US Army Natick Research and Development Command ATTN: DRDNA-DT, D. Sieling Natick, MA 01762
1	Commander US Army Tank Automotive Research and Development Command ATTN: DRDTA-UL Warren, MI 48090
1	US Army Tank Automotive Materiel Readiness Command ATTN: DRSTA-CG Warren, MI 48090
1	Project Manager Improved TOW Vehicle ATTN: DRCPM-ITV US Army Tank Automotive Research & Development Command Warren, MI 48090
1	Program Manager M1 Abrams Tank System ATTN: DRCPM-GMC-SA Warren, MI 48090
1	Project Manager Fighting Vehicle Systems ATTN: DRCPM-FVS Warren, MI 48090
1	Director US Army TRADOC Systems Analysis Activity ATTN: ATAA-SL, Tech Lib White Sands Missile Range, NM 88002
1	Project Manager M-60 Tank Development ATTN: DRCPM-M60TD Warren, MI 48090
1	Commander US Army Training & Doctrine Command ATTN: ATCD-MA/ MAJ Williams Fort Monroe, VA 23651
2	Commander US Army Materials and Mechanics Research Center ATTN: DRXMR-ATL Tech Library Watertown, MA 02172

DISTRIBUTION LIST

No. Of Copies	Organization
1	Commander US Army Research Office ATTN: Tech Library P. O. Box 12211 Research Triangle Park, NC 27709
1	Commander US Army Mobility Equipment Research & Development Command ATTN: DRDME-WC Fort Belvoir, VA 22060
1	Commander US Army Logistics Mgmt Ctr Defense Logistics Studies Fort Lee, VA 23801
2	Commandant US Army Infantry School ATTN: Infantry Agency Fort Benning, GA 31905
1	US Army Armor & Engineer Board ATTN: STEBB-AD-S Fort Knox, KY 40121
1	Commandant US Army Aviation School ATTN: Aviation Agency Fort Rucker, AL 36360
1	Commandant Command and General Staff College Fort Leavenworth, KS 66027
1	Commandant US Army Special Warfare School ATTN: Rev & Tng Lit Div Fort Bragg, NC 28307
1	Commandant US Army Engineer School ATTN: ATSE-CD Ft. Belvoir, VA 22060
1	Commander US Army Foreign Science & Technology Center ATTN: DRXST-MC-3 220 Seventh Street, NE Charlottesville, VA 22901
1	President US Army Artillery Board Ft. Sill, OK 73504
2	Commandant US Army Field Artillery School ATTN: ATSF-CO-MW, B. Willis Ft. Sill, OK 73503
3	Commandant US Army Armor School ATTN: ATZK-CD-MS/ M. Falkovitch Armor Agency Fort Knox, KY 40121
1	Chief of Naval Materiel Department of the Navy ATTN: J. Amlie Washington, DC 20360
1	Office of Naval Research ATTN: Code 473, R. S. Miller 800 N. Quincy Street Arlington, VA 22217
2	Commander Naval Sea Systems Command ATTN: SEA-62R2, J. W. Murrin R. Beauregard National Center, Bldg. 2 Room 6E08 Washington, DC 20362
1	Commander Naval Air Systems Command ATTN: NAIR-954-Tech Lib Washington, DC 20360

DISTRIBUTION LIST

No. Of Copies	Organization
1	Strategic Systems Project Office Dept. of the Navy Room 901 ATTN: J. F. Kincaid Washington, DC 20376
1	Assistant Secretary of the Navy (R, E, and S) ATTN: R. Reichenbach Room 5E787 Pentagon Bldg. Washington, DC 20350
1	Naval Research Lab Tech Library Washington, DC 20375
5	Commander Naval Surface Weapons Center ATTN: Code G33, J. L. East D. McClure W. Burrell J. Johndrow Code DX-21 Tech Lib Dahlgren, VA 22448
2	Commander US Naval Surface Weapons Center ATTN: J. P. Consaga C. Gotzmer Indian Head, MD 20640
4	Commander Naval Surface Weapons Center ATTN: S. Jacobs/Code 240 Code 730 K. Kim/Code R-13 R. Bernecker Silver Spring, MD 20910
2	Commanding Officer Naval Underwater Systems Center Energy Conversion Dept. ATTN: CODE 5B331, R. S. Lazar Tech Lib Newport, RI 02840
4	Commander Naval Weapons Center ATTN: Code 388, R. L. Derr C. F. Price T. Boggs Info. Sci. Div. China Lake, CA 93555
2	Superintendent Naval Postgraduate School Dept. of Mechanical Engineering ATTN: A. E. Fuhs Code 1424 Library Monterey, CA 93940
6	Commander Naval Ordnance Station ATTN: P. L. Stang J. Birkett S. Mitchell C. Christensen D. Brooks Tech Library Indian Head, MD 20640
1	AFSC Andrews AFB Washington, DC 20331
1	Program Manager AFOSR Directorate of Aerospace Sciences ATTN: L. H. Caveny Bolling AFB, DC 20332
6	AFRPL (DYSC) ATTN: D. George J. N. Levine B. Goshgarian D. Thrasher N. Vander Hyde Tech Library Edwards AFB, CA 93523

DISTRIBUTION LIST

No. Of Copies	Organization
1	AFFTC ATTN: SSD-Tech Lib. Edwards AFB, CA 93523
1	AFATL ATTN: DLYV Eglin AFB, FL 32542
1	AFATL/DLDL ATTN: O. K. Heiney Eglin AFB, FL 32542
1	ADTC ATTN: DLODL Tech Lib Eglin AFB, FL 32542
1	AFFDL ATTN: TST-Lib Wright-Patterson AFB, OH 45433
1	HQ NASA 600 Independence Avenue, SW ATTN: Code JM6, Tech Lib. Washington, DC 20546
1	NASA/Lyndon B. Johnson Space Center ATTN: NHS-22, Library Section Houston, TX 77058
1	Aerodyne Research, Inc. Bedford Research Park ATTN: V. Yousefian Bedford, MA 01730
1	Aerojet Solid Propulsion Co. ATTN: P. Micheli Sacramento, CA 95813
1	AVCO Everett Rsch Lab ATTN: D. Stickler 2385 Revere Beach Parkway Everett, MA 02149
2	Calspan Corporation ATTN: E. B. Fisher Tech Library P. O. Box 400 Buffalo, NY 14225
1	Foster Miller Associates ATTN: A. Erickson 135 Second Avenue Waltham, MA 02154
1	Atlantic Research Corp. ATTN: M. K. King 5390 Cherokee Avenue Alexandria, VA 22314
1	General Applied Sciences Lab ATTN: J. Erdos Merrick & Stewart Avenues Westbury Long Island, NY 11590
1	General Electric Company Armament Systems Dept. ATTN: M. J. Bulman Room 1311 Lakeside Avenue Burlington, VT 05412
1	Hercules Powder Co. Allegheny Ballistics Laboratory ATTN: R. B. Miller P. O. Box 210 Cumberland, MD 21501
1	Hercules, Inc Bacchus Works ATTN: K. P. McCarty P. O. Box 98 Magna, UT 84044

DISTRIBUTION LIST

No. Of Copies	Organization
1	Hercules, Inc. Eglin Operations AFATL DLDL ATTN: R. L. Simmons Eglin AFB, FL 32542
1	IITRI ATTN: M. J. Klein 10 W. 35th Street Chicago, IL 60616
2	Lawrence Livermore Laboratory ATTN: M. S. L-355, A. Buckingham M. Finger P. O. Box 808 Livermore, CA 94550
1	Olin Corporation Badger Army Ammunition Plant ATTN: R. J. Thiede Baraboo, WI 53913
1	Olin Corporation Smokeless Powder Operations ATTN: R. L. Cook P. O. Box 222 ST. Marks, FL 32355
1	Paul Gough Associates, Inc. ATTN: P. S. Gough P. O. Box 1614 Portsmouth, NH 03801
1	Physics International Company 2700 Merced Street Leandro, CA 94577
1	Princeton Combustion Research Lab., Inc. ATTN: M. Summerfield 1041 US Highway One North Princeton, NJ 08540
1	Pulsepower Systems, Inc. ATTN: L. C. Elmore 815 American Street San Carlos, CA 94070
2	Rockwell International Rocketdyne Division ATTN: BA08 J. E. Flanagan J. Grey 6633 Canoga Avenue Canoga Park, CA 91304
1	Science Applications, Inc. ATTN: R. B. Edelman 23146 Cumorah Crest Woodland Hills, CA 91364
1	Scientific Research Assoc., Inc. ATTN: H. McDonald P. O. Box 498 Glastonbury, CT 06033
1	Shock Hydrodynamics, Inc. ATTN: W. H. Andersen 4710-16 Vineland Avenue North Hollywood, CA 91602
3	Thiokol Corporation Huntsville Division ATTN: D. Flanigan R. Glick Tech Library Huntsville, AL 35807
2	Thiokol Corporation Wasatch Division ATTN: J. Peterson Tech Library P. O. Box 524 Brigham City, UT 84302
2	Thiokol Corporation Elkton Division ATTN: R. Biddle Tech Lib. P. O. Box 241 Elkton, MD 21921

DISTRIBUTION LIST

No. Of Copies	Organization
2	United Technologies Chemical Systems Division ATTN: R. Brown Tech Library P. O. Box 358 Sunnyvale, CA 94086
1	Universal Propulsion Company ATTN: H. J. McSpadden Black Canyon Stage 1 Box 1140 Phoenix, AZ 85029
1	Southwest Research Institute Institute Scientists ATTN: Robert E. White 8500 Culebra Road San Antonio, TX 78228
1	Battelle Memorial Institute ATTN: Tec Library 505 King avenue Columbus, OH 43201
1	Brigham Young University Dept. of Chemical Engineering ATTN: M. Beckstead Provo, UT 84601
1	California Institute of Tech 204 Karman Lab Main Stop 301-46 ATTN: F. E. C. Culick 1201 E. California Street Pasadena, CA 91125
1	California Institute of Tech Jet Propulsion Laboratory ATTN: L. D. Strand 4800 Oak Grove Drive Pasadena, CA 91103
1	University of Illinois Dept. of Mech. Eng. ATTN: H. Krier 144 MEB, 1206 W. Green Street Urbana, IL 61801
1	University of Massachusetts Dept. of Mechanical Engineering ATTN: K. Jakus Amherst, MA 01002
1	University of Minnesota Dept. of Mechanical Engineering ATTN: E. Fletcher Minneapolis, MN 55455
1	Case Western Reserve University Division of Aerospace Sciences ATTN: J. Tien Cleveland, OH 44135
3	Georgia Institute of Tech School of Aerospace Eng. ATTN: B. T. Zinn E. Price W. C. Strahle Atlanta, GA 30332
1	Institute of Gas Technology ATTN: D. Gidaspow 3424 S. State Street Chicago, IL 60616
1	Johns Hopkins University Applied Physics Laboratory Chemical Proplsion Information Agency ATTN: T. Christian Johns Hopkins Road Laurel, MD 20707
1	Massachusetts Institute of Tech Dept of Mechanical Engineering ATTN: T. Toong Cambridge, MA 02139

DISTRIBUTION LIST

No. Of Copies	Organization
1	Pennsylvania State University Applied Research Lab ATTN: G. M. Faeth P. O. Box 30 State College, PA 16801
1	Pennsylvania State University Dept. Of Mechanical Engineering ATTN: K. Kuo University Park, PA 16802
1	Purdue University School of Mechanical Engineering ATTN: J. R. Osborn TSPC Chaffee Hall West Lafayette, IN 47906
1	Rensselaer Polytechnic Inst. Department of Mathematics Troy, NY 12181
1	Rutgers University Dept. of Mechanical and Aerospace Engineering ATTN: S. Temkin University Heights Campus New Brunswick, NJ 08903
1	SRI International Propulsion Sciences Division ATTN: Tech Library 333 Ravenswood Avenue Menlo Park, CA 94025
1	Stevens Institute of Technology Davidson Laboratory ATTN: R. McAlevy, III Hoboken, NJ 07030
2	Los Alamos Scientific Lab ATTN: T. D. Butler, MS B216 M. Division, B. Craig P. O. Box 1663 Los Alamos, NM 87545
1	University of Southern California Mechanical Engineering Dept. ATTN: OHE200, M. Gerstein Los Angelos, CA 90007
2	University of Utah Dept. of Chemical Engineering ATTN: A. Baer G. Flandro Salt Lake City, UT 84112
1	Washington State University Dept. of Mechanical Engineering ATTN: C. T. Crowe Pullman, WA 99164

Aberdeen Proving Ground

Dir, USAMSAA
ATTN: DRXSY-D
DRXSY-MP, H. Cohen
Cdr, USATECOM
ATTN: DRSTE-TO-F
STEAP-MT, S. Walton
G. Rice
D. Lacey
C. Herud
Dir, HEL
ATTN: J. Weisz
Dir, USACSL, Bldg. E3516, EA
ATTN: DRDAR-CLB-PA
DRDAR-ACW